R

325

4-4-61

IDO - 14540

MASTER

CHEMICAL PROCESSING TECHNOLOGY
QUARTERLY PROGRESS REPORT
July - September, 1960

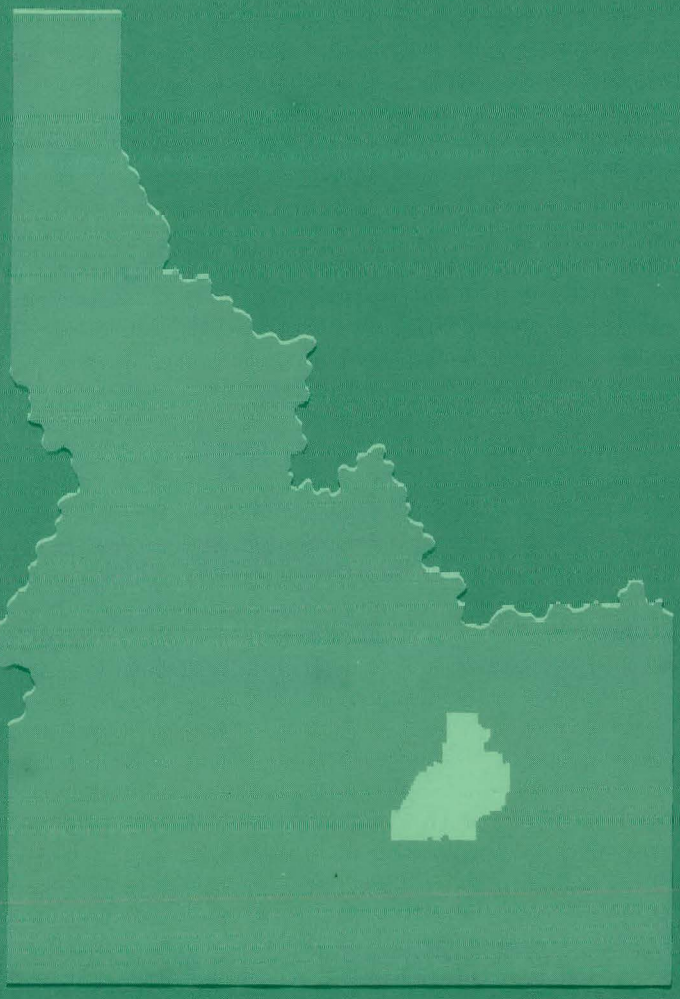

PHILLIPS PETROLEUM COMPANY

ATOMIC ENERGY DIVISION

NATIONAL REACTOR TESTING STATION

US ATOMIC ENERGY COMMISSION

DISCLAIMER

PRICE $1.50

Available from the
Office of Technical Services
U. S. Department of Commerce
Washington 25, D. C.

LEGAL NOTICE

Printed in USA

PAGES 1 to 2

WERE INTENTIONALLY

LEFT BLANK

IDO-14540
AEC Research and Development Report
General, Miscellaneous, and Progress Reports
TID-4500 (16th Ed.)

CHEMICAL PROCESSING TECHNOLOGY

QUARTERLY PROGRESS REPORT

July - September 1960

Submitted: February 15, 1961
Issued: February 28, 1961

J. R. Huffman
Assistant Manager, Technical

J. A. McBride
Technical Director

C. M. Slansky
Chemical Development

F. M. Warzel
Process Development

J. R. Bower
Editor

PHILLIPS PETROLEUM COMPANY
Atomic Energy Division
Idaho Falls, Idaho
Contract AT(10-1)-205

U. S. ATOMIC ENERGY COMMISSION - IDAHO OPERATIONS OFFICE

Previous Reports in Series:

IDO-14324
IDO-14337
IDO-14350
IDO-14354
IDO-14362
IDO-14364
IDO-14383
IDO-14385
IDO-14391
IDO-14400
IDO-14410
IDO-14419
IDO-14422
IDO-14430
IDO-14443
IDO-14453
IDO-14457
IDO-14467
IDO-14471
IDO-14494
IDO-14509
IDO-14512
IDO-14514
IDO-14520
IDO-14526
IDO-14530
IDO-14534

CHEMICAL PROCESSING TECHNOLOGY

QUARTERLY PROGRESS REPORT
JULY - SEPTEMBER 1960

TABLE OF CONTENTS

LIST OF TABLES

LIST OF FIGURES

LIST OF FIGURES (Continued)

CHEMICAL PROCESSING TECHNOLOGY

QUARTERLY PROGRESS REPORT
JULY - SEPTEMBER 1960

J. R. Bower, Editor

I. SUMMARY

The Idaho Chemical Processing Plant did not process spent fuel during this period because the recovery plant was shut down for decontamination, minor modification and repair, and change-over in the processing program. Certain liquid wastes in permanent storage were recycled and further concentrated to conserve waste storage space. Barium-140 production proceeded on schedule without incident, achieving good recovery of high quality product. Preparations were underway for startup testing of the Demonstrational Waste Calcining Facility, construction of which is nearing completion. Progress is reported on the use of a packed steam stripper to free waste solvent from low concentrations of plutonium prior to incineration.

Aqueous zirconium processing studies directed at reduction of solution volumes to be processed and stored as waste, indicate that precipitation of barium fluozirconate from dissolver solutions (to permit processing of a concentrated uranium solution) is preferably carried out using mixtures of barium hydroxide or barium fluoride with barium nitrate, thus achieving better zirconium separation (94%), lower uranium loss (0.3%), and better definition of fission product behavior (strontium and cerium carry quantitatively with the precipitate) than when barium nitrate alone is used as the precipitant. With low acidity favoring high zirconium recovery, barium hydroxide offers the advantage of neutralizing excess acid while supplying barium for the precipitation, and barium fluoride permits adjustment of the F - Zr ratio without acid addition while also supplying barium.

Continued studies on the dissolution of ceramic fuels (beryllium oxide-uranium oxide) in molten ammonium bifluoride have demonstrated that a true solution of uranium is not achieved in the reagent, but that the dispersion obtained will pass through a 20 micron filter and is readily dissolved in nitric acid for further processing. An activation energy of 3.78 Kcal/mole for the dissolution of beryllium oxide in ammonium bifluoride has been derived from dissolution rate data presented for several different temperatures.

Summarized conclusions of a topical report on solvent stability include the finding that extracted zirconium degrades tributyl phosphate approximately one thousand times faster than extracted nitric acid, an item of special significance in light of the quantities of fission product zirconium encountered in high burnup fuels.

Completion of a study on evaporation and mixing in a large diameter vessel packed with Raschig rings, to simulate a possible means of criticality control in a non-geometrically safe vessel through uniform interior distribution of neutron absorbing materials, indicated acceptable, if not ideal, performance in these operations.

Pilot plant studies of the fluidized bed calcination process for reduction of radioactive liquid wastes to the more easily stored solid form have continued with investigation of the operating characteristics, in the two-foot square calciner, of one of the feed spray nozzles intended for use in the Demonstrational Waste Calcining Facility. Runs of 8 days' duration demonstrated that a liquid feed rate of at least 120 l/hr through one spray nozzle could be maintained without inducing caking of the product or causing noticeable temperature fluctuations in the bed beyond a distance of 12 to 15 inches from the nozzle, measured along the axial center line of the spray pattern. Tests were limited to this maximum rate by capacity of the laboratory compressors supplying fluidizing and nozzle (atomizing) air; at very low nozzle air-to-liquid volume ratios, particle growth increased, resulting in a bed of relatively large particles with poor heat transfer from the NaK tubes to the bed. Attrition of the calcined product, as estimated from the quantity of fines carried in the off gas from the calciner, was influenced to the greatest extent by the nozzle atomizing air (as a result of a high-velocity jet grinding action), and to a considerably smaller extent by fluidizing air velocity and liquid feed injection rates. Rapid erosion of the flat titanium nozzle face (0.86 inches/year) during these tests led to study of nozzle tip designs and development of an extended cone tip, less susceptible to wear by impingement of alumina particles under the influence of an air vortex.

The physical structure of the alumina produced during operation of the fluidized bed calciner has, for unknown reasons, rapidly shifted between an amorphous and a predominantly alpha-crystalline form. Examination of bulk product produced in the pilot plant, fines carried in the off gas, and dissected particles (produced under both high and low alpha alumina forming conditions) demonstrated that in every case the fines elutriated from the calciner had a lower alpha alumina content than the bulk product or any part of an individual dissected calcine particle. The data indicated that material which is spray dried directly from the nozzle (and more readily carried in the gas stream because of its small size) is predominantly amorphous, while that deposited on calcine particles can either remain largely amorphous or be rapidly converted to the alpha form under conditions not yet understood. Preliminary laboratory investigations have led to partial conversion (5 to 65 per cent) of amorphous alumina to alpha alumina under influence of high temperature for prolonged periods (192 hours at 927°C), and more especially in the presence of relatively high concentrations of sodium nitrate and nitric acid, but have not yet resulted in significant conversion under the temperature conditions (400 to 500°C) prevailing in the calciner. Development of a method for determining calcine particle density by a mercury displacement technique has furnished a factor required in elutriation (bed depletion) calculations and made possible the calculation of intra-particle porosity, a basic property of the alumina not heretofore known.

Examination of the major components of the pilot plant calciner and NaK heater for corrosion damage after approximately 6000 hours' service, the major portion of which was at 1000 to 1440°F, indicated satisfactory service from the materials of construction (type 316 stainless steel for the liquid NaK tube bundle in the oil-fired furnace and Carpenter 20 for the fluidized bed heat exchanger and calciner body), with a maximum rate of corrosion of 2 mils per month for the liquid NaK furnace bundle.

Laboratory studies have led to selection of optimum ranges of certain reaction conditions for the calcination of fluoride-containing waste solutions (e.g., from zirconium fuel processing) to give minimum volatilization of fluoride (a corrosion-inducing agent) and minimum leachability of the calcine (a storage containment problem). Data are presented in support of the following conditions: calcination temperature near 500°C; CaO/F equivalency ratio of 0.75 to 1.0; aluminum concentration above 0.3M; nitrate concentrations either below 2N or above 3N. Other areas remain to be explored before a complete recommendation can be made for utilization of this process. It is hoped that fluoride volatility can be held to a sufficiently low value to permit calcination of STR-type wastes in the DWCF.

In further study of the concentration and fixation of radioactive wastes to develop cheaper and easier means of disposal or storage of wastes, it has been found that an exchange bed of ammonium phosphomolybdate (APM) supported on silica gel shows a decontamination factor of approximately 3,000 for Cs-137 in aluminum nitrate-nitric acid solution, and a capacity of 35 mg of cesium per gram of APM. An attempt to fix the activity in calcined alumina containing Cs-137, by immersing the particles in molten aluminum and then cooling, resulted in a solid from which the activity was still leachable although very slowly (40% in 700 hours) as compared with the rate from uncoated alumina (70% in 1 hour). In other experiments it was demonstrated that silica gel could be used to absorb a liquid waste and the waste calcined in situ. By repeated absorption-calcination cycles, a waste containing 2M aluminum nitrate was concentrated fivefold without plugging the pores between the silica gel granules in a fixed bed.

A program of preparation and measurement of properties of pure compounds of calcium, zirconium, fluorine, and oxygen, initiated to furnish basic data for the zirconium-fluoride waste precipitation-calcination program, led to preparation, identification and description of X-ray diffraction patterns for two hitherto unreported compounds, calcium fluozirconate ($CaZrF_6 \cdot (2\text{-}3)H_2O$) and strontium fluozirconate ($SrZrF_6$). This could be significant in development of a process for isolation of strontium from wastes by precipitation in a similar manner.

In an investigation of the practical aspects of removal, by mercury cathode electrolysis, of iron, nickel, and chromium from waste solutions resulting from processing of stainless steel reactor fuels, it was demonstrated that up to 3 per cent iron or nickel could be electrolyzed into the mercury before the amalgam reached a semi-solid state which would require treatment to remove the base metals. A maximum of 0.3 per cent chromium was taken up before electrolysis ceased and a fine black powder separated from the mercury.

Electrolytic dissolution in nitric acid was demonstrated to be applicable to a wide variety (26 specimens examined) of stainless steel and other alloy materials. Concentrations of 75 g/liter of most of these metals were easily obtained at high current efficiencies; Duriron and Durichlor were exceptions but could, presumably, have also been dissolved using longer dissolution times. Silicon and molydenum contributed to excess anode sludge formation but, in general, the amounts of residue remaining were not intolerable. Continuous dissolution of a variety of stainless steel shapes, without interference to the electrolytic action through formation of insulating films, has been accomplished through use of a tamping device which periodically applies a sudden mechanical pressure to the contents of the dissolver, thus breaking down any "valve metal" film and maintaining electrical contact. Electrolytic cutting of stainless steel, through use of a "cathodic" needle which delivers a fine stream of electrolyte against the "anodic" fuel section, has been demonstrated. Since the products of the cut are dissolved electrochemically, the problem of contamination by chips and dust, associated with mechanical shearing or sawing of fuel elements, is avoided.

Fundamental information on the effect of cell and electrode geometry on such factors as electrolytic resistance and current density distribution during electrolytic dissolution is being obtained; such important factors as speed and uniformity of dissolution, with minimization of undesirable side effects due to local current density variations, and dissipation of energy related to resistance are involved. In a study of anode basket hole area and arrangement, and anode-cathode spacing, relationships are specified which should result in the average current being not less than 90% of the maximum current on the cathode, and the resistance between the anode and cathode being not greater than three times the value obtainable if no basket were interposed. Anode basket holes in a triangular array have a slight advantage (less than 10%) over holes in a square array.

Reasonable corrosion resistance of a Carpenter 20 cathode (less than 20 mils per month) was demonstrated as long as the solution acid and nitrate concentrations were kept above certain designated minimums. At higher current densities, higher acid and nitrate concentrations are required, e.g., at 1.5 amps/cm^2, acid must be $>3\underline{M}$ and nitrate $>6\underline{M}$.

Collection of basic data on the electrolytic dissolution of zirconium in HCl-methanol has continued with development of an equation summarizing all the data obtained on the potential-current density relationships as functions of temperature and HCl concentration.

Several aspects of the ARCO process, which employs molten lead chloride as a solvent for reactor fuel alloys, have received further attention. Use of HCl as a leaching agent to recover uranium from the salt matrix has proved unsatisfactory because of high residual losses (5 to 15%); nitric acid remains the most satisfactory leaching agent with an average uranium loss of only 0.04%. Results to date have been inconclusive in determination of the behavior of fission product niobium in the process. Uranium oxide (UO_2), in the form of pellets from an unirradiated PWR fuel pin, was essentially insoluble in molten lead

chloride, suggesting the possibility of using the ARCO process as a decladding step for zirconium or Zircaloy-clad fuel elements. Additional static corrosion tests, in the lead-chloride system at 528°C, indicated Haynes 21 alloy to have a fair resistance to attack, with a corrosion rate of 1.1 to 1.4 mils per month, although there was a certain amount (unevaluated) of localized attack.

II. ICPP OPERATIONAL SCHEDULE, PERFORMANCE AND PROBLEMS

A. ICPP Processing Schedule, J. R. Bower

The Idaho Chemical Processing Plant was not operating on fuel recovery during this quarter. The reprocessing equipment was shut down and undergoing decontamination to permit making certain desirable changes to pumping and evaporating equipment since the fuel supply awaiting reprocessing in the storage basin had been reduced, during the previous quarter, to a level making further processing impractical until the inventory once again built up.

Concentration of the contents of a 300,000 gallon waste storage tank containing second and third cycle extraction wastes and miscellaneous process equipment wastes has started. The solution is being recycled through the process equipment waste evaporator with the concentrate, which will be reduced to approximately 180,000 gallons, being redirected to permanent waste, thus recovering approximately 120,000 gallons of storage space valued at approximately $240,000. For varied reasons during past operations, including temporary departure from flowsheet conditions for operational reasons, jet dilutions during transfers, non-flowsheet conditions during startup, testing or decontamination, and jetting of water-filled sumps, the contents of this tank were at a lower concentration than necessary for stability according to laboratory tests. The possibility of further concentrating other waste materials now in storage is being studied.

Operations emphasis has been on preparations for startup of the Demonstrational Waste Calcining Facility. Functional tests were being conducted as rapidly as individual pieces of equipment were made available by the construction contractor. Work was continued on preparation of preliminary operating procedures, data sheets, calibration curves, calculation methods, etc.

Three barium-140 product runs were completed without incident. Product recovery was as listed in Table 1.

TABLE 1

BARIUM-140 PRODUCTION AT ICPP, JULY - SEPTEMBER, 1960

Run No.	Curies	Per Cent Recovery
044	Run cancelled at customer's request.	
045	30,600	54.8
046	29,324	61.8
047	16,200	56.0

B. Plutonium Contamination of Solvent, H. V. Chamberlain, Problem Leader; C. R. Ford

A problem in ICPP operations has been the control of plutonium alpha activity from the waste solvent incinerator. Previous studies(1,2,3) of this problem have shown that neither passing the waste solvent (before burning) over activated carbon nor treating of the waste solvent with ferrous sulfamate will, by itself, dependably decrease the activity released from the incinerator to a desirable level. Since laboratory tests have indicated that both ionic and non-ionic species of plutonium may be present in the waste solvent, the consecutive application of both of the above operations would probably produce the desired result. However, a superior alternative appears to be the use of a packed, steam stripping column to volatilize the bulk of the solvent while maintaining a small flow from the bottom of the stripper to carry the essentially non-volatile plutonium compounds.

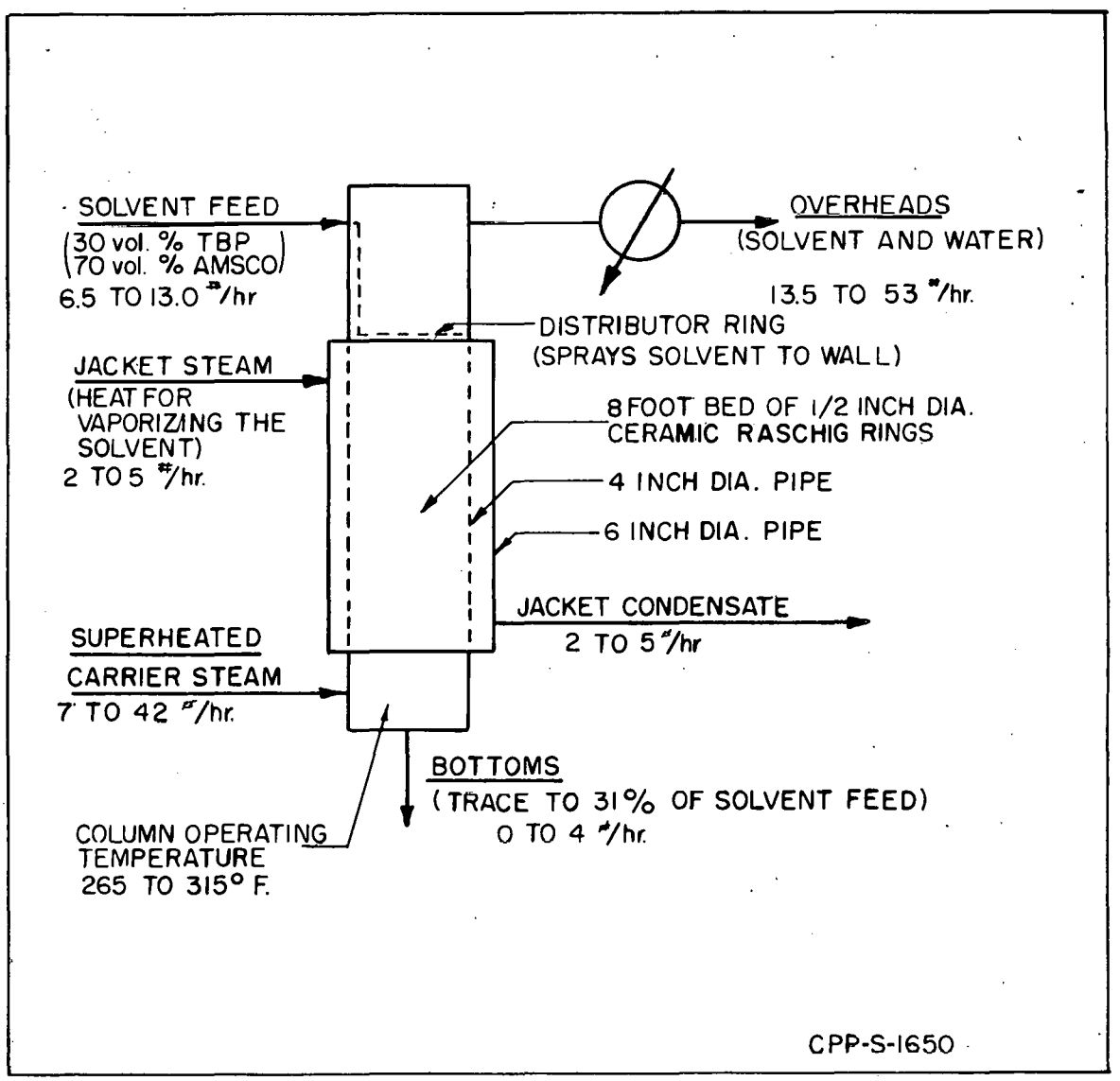

Figure 1 - Schematic Diagram of Pilot Plant Experimental Steam Stripper System

A program has been initiated to study the feasibility of steam stripping a TBP-Amsco solution in a packed column. The study is being conducted in the Cold Pilot Plant using an uncontaminated solvent feed (30 volume per cent TBP, 70 volume per cent Amsco 120-90W without plutonium or fission products present).

The goal of this study is the determination of the carrier-steam to solvent-feed mass ratio, temperature, and height of bed packing required to vaporize 98 to 99 per cent of the solvent feed. A schematic diagram of the equipment used for pilot plant studies is shown in Figure 1. The data obtained from this column will be extrapolated to design a packed steam stripper for ICPP use with the contaminated waste solvent.

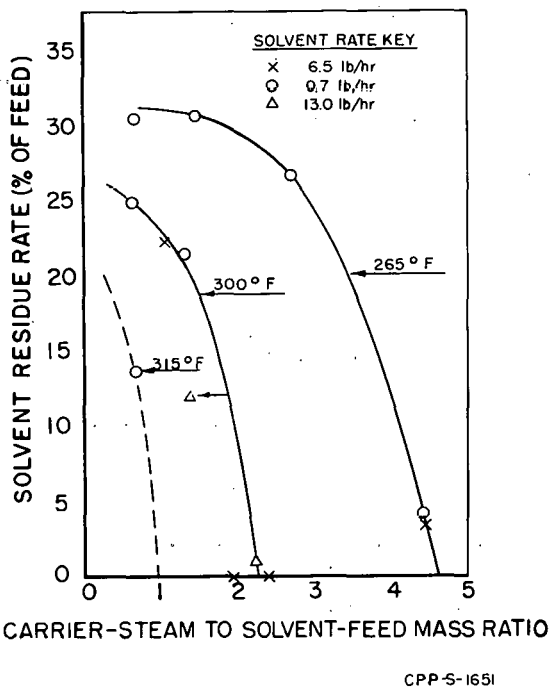

Fig. 2 - Effect of Carrier Steam Rate and Column Temperature on Solvent Residue Rate
Column Diameter - 4 in
Height of packed section - 8 ft
Raschig ring packing size-1/2 in

Pilot plant data have been obtained using an eight-foot high by four-inch diameter packed bed at solvent feed rates of 6.5, 9.7, and 13.0 pounds per hour; carrier steam rates of 7, 14, 28, and 42 pounds per hour; and column temperatures of 265, 300 and 315°F. These data are presented in Figure 2; they indicate that the carrier-steam to solvent-feed mass ratio required to limit the residue rate from the bottom of the steam stripper to approximately one per cent of the solvent feed decreased from 4.6 to 2.2 when the column operating temperature was increased from 265 to 300°F. Increasing the solvent feed rate from 6.5 to 13.0 pounds per hour on these tests did not change the required carrier-steam to solvent-feed mass ratio. One run has been completed at a column temperature of 315°F; this indicates that a carrier-steam to solvent-feed mass ratio of approximately one is required to obtain a residue rate of one per cent at 315°F.

Additional runs are planned at 300°F with a bed height of four feet and TBP concentrations of five and thirty per cent.

C. Corrosion in TURCO 55-8A, N. D. Stolica, Problem Leader; T. L. Hoffman

An accelerated scoping corrosion study was conducted on welded and unwelded wrought stainless steel type 347 (Cb and Ta) and titanium 55A in 5.9 per cent TURCO 55-8A, a commercial decontaminating agent. Testing conditions involved immersing specimens of these alloys into the boiling TURCO solution for 48 hours. Results from this preliminary work indicate that both stainless steel type 347 and titanium 55A suffer very feeble attack. The observed maximum corrosion rates were about 0.1 mil per month.

III. AQUEOUS PROCESSING STUDIES

Section Chiefs: K. L. Rohde, Process Chemistry
H. T. Hahn, Chemical Research
J. A. Buckham, Technical Projects

The process in use at the ICPP for recovering uranium from uranium-zirconium alloy fuels utilizes hydrofluoric acid as dissolvent and aluminum nitrate to complex the fluoride ion prior to solvent extraction. New processes are under development in an effort to reduce waste volumes, obtain less corrosive process streams, handle alloys of higher uranium content and increase process equipment capacity.

The alloy fuels under consideration are 95 to 99 per cent zirconium; the extraction process capacity is limited by the requirement for handling this large volume of zirconium (a diluent of the uranium), and extraction raffinates generated in correspondingly large volume involve an expensive storage problem. A head-end precipitation of the zirconium and fluoride from the STR dissolver solution as barium fluozirconate has been demonstrated in the laboratory and results in low uranium losses to the washed precipitate[4]. This research has been continued to determine the path of fission products during the precipitation of barium fluozirconate. Distribution of major fission products between precipitates and filtrates is given for several flowsheets.

After the precipitation of barium fluozirconate, it will probably be desirable to evaporate the solution to smaller volumes. Corrosion studies are described in which both Carpenter 20 and type 347 stainless steel, potential materials of construction for an evaporator, showed severe intergranular and preferential weld attack. Aluminum nitrate may reduce the attack by complexing any remaining fluoride ion.

Study of the molten ammonium bifluoride (MAB) process for dissolving beryllium oxide-uranium oxide ceramic fuels showed that only part of the uranium dissolved in the MAB; a majority remained in a suspended solid phase. Process difficulties are not anticipated as a result of this since the uranium is readily dissolved in nitric acid in a following step.

Results of work which has been in progress for some time[3,5] on the effect of extracted zirconium and nitric acid upon the chemical stability of tributyl phosphate (TBP) extraction solvent are summarized in reference to a topical report which is in preparation[6]. Extracted zirconium was found to degrade TBP approximately one thousand times faster than extracted nitric acid, an item of special significance in light of the quantities of fission product zirconium encountered in high burnup fuels.

Completion of a study on evaporation and mixing in a large diameter vessel packed with Raschig rings, to simulate a possible means of criticality control in a non-geometrically safe vessel through uniform interior distribution of neutron absorbing materials, indicated that these operations could be satisfactorily performed although, admittedly, with some interference caused by the ring packing.

A. Aqueous Zirconium Fuel Processing

1. Barium Fluozirconate Precipitation Process:
J. W. Codding, Problem Leader; B. J. Newby

Removal of zirconium from STR dissolver solutions, by precipitation as barium fluozirconate in a head-end process, results in a decrease in column feed volumes by permitting concentration of the feed without jeopardizing the stability of the process solutions; thus, an important decrease in waste volume can be accomplished. Three flowsheets have been proposed[4] to accomplish zirconium and fluoride removal as barium fluozirconate. Scoping studies to define fission product behavior during the precipitation of barium fluozirconate from STR dissolver solutions, following variations of these three flowsheets, are reported.

a. Experimental

The STR dissolver solutions used in this work were prepared by diluting Idaho Chemical Processing Plant first cycle STR extraction waste 50 times with radioactively cold, simulated STR dissolver solution. The latter solution was made by dissolving uranium-zirconium alloy in sufficient hydrofluoric acid to give a 4.5 or 5 to 1 mole ratio of fluoride to zirconium. Hydrogen peroxide was added to oxidize the uranium and to avoid precipitation of uranium tetrafluoride. The solution with a 4.5 to 1 fluoride-zirconium mole ratio contained 1.6M zirconium, and 0.9N acid; the solution with a 5 to 1 fluoride-zirconium mole ratio contained 1.7M zirconium and 1.8N acid.

Precipitations were made in a 300 ml partially-capped graduated cylinder fabricated from polypropylene and equipped with a mechanically driven Teflon stirrer. Fifty ml of STR dissolver solution were put into the vessel, the solution adjusted to give the appropriate fluoride to zirconium mole ratio, and the precipitant added. The cylinder was submerged to about the 100 ml mark in a covered water bath and heated at 94°C while stirring for 2 hours. The upper portion of the cylinder was cooled by an air jet during the precipitation step, to prevent excessive escape of condensible vapors, while evaporation losses were continually replaced by water addition. After cooling the resultant slurry to room temperature, the residue was vacuum filtered, washed four times with 25 ml of 0.1N nitric acid, and dissolved in nitric acid-boric acid. The filtrate, washed solution, and dissolved residue were analyzed for the appropriate macro-constituents and fission products.

b. Results and Conclusions

The behavior of Sr^{89-90}, Cs^{137}, Ce^{144}, and Ru^{106} under various precipitation conditions is summarized in Table 2. When either solid barium fluoride or barium hydroxide was used with solid barium nitrate as the precipitant (flowsheets c, d, e, Table 2) the behavior of these fission products was well defined; fission product behavior was not well defined when solid barium nitrate alone was used as the precipitant (flowsheets a and b).

TABLE 2

FISSION PRODUCT BEHAVIOR DURING PRECIPITATION OF
BARIUM FLUOZIRCONATE FROM STR DISSOLVER SOLUTIONS

Flowsheet	Original Dissolver Solution Composition	Process Component	Material Distribution (per cent by weight)							
			Zr	U	Gross Gamma	Gross Beta	Sr^{89-90}	Ce^{144}	Cs^{137}	Ru^{106}
(a)	(f)	Filtrate	8.5	80	42	26	6	24	67	86
		Wash Soln.	8.5	19	12	9	8	7	17	13
		Precipitate	83	0.9	46	65	86	69	16	1
(b)	(f)	Filtrate	23	69	--	--	--	--	--	--
		Wash Soln.	7.7	29	--	--	--	--	--	--
		Precipitate	70	2.4	--	---	--	--	--	--
(b)	(f)	Filtrate	21	--	--	--	--	--	--	--
		Wash Soln.	5	--	--	--	--	--	--	--
		Precipitate	74	--	--	--	--	--	--	--
(c)	(f)	Filtrate	7.6	66	21	9	3	1	54	66
		Wash Soln.	5.8	34	12	5	1	0.5	32	33
		Precipitate	87	0.3	67	86	96	98.5	14	1
(d)	(f)	Filtrate	4.7	53	16	6	0.1	0.01	37	58
		Wash Soln.	7.4	46	18	7	0.2	0.05	41	41
		Precipitate	88	0.6	66	87	99	99.9	22	1
(e)	(g)	Filtrate	5.8	57	24	6	0.1	0.01	38	57
		Wash Soln.	7.3	43	20	1	0.2	0.01	38	42
		Precipitate	87	0.3	56	93	99	99.98	24	1

(a) 21.8 of sclid $Ba(NO_3)_2$ was added to 50 ml of dissolver solution; the slurry was stirred at 94°C for 2 hours.

(b) 3 ml of 48% HF was added to 50 ml of dissolver solution giving it a F - Zr mole ratio of 6 to 1; 21.8 g. of solid $Ba(NO_3)_2$ was added to the dissolver solution; the slurry was stirred at 94°C for 2 hours.

(c) 3 ml of 48% HF was added to 50 ml of dissolver solution giving it a F - Zr mole ratio of 6 to 1; 22.9 g. of $Ba(OH)_2 \cdot 8H_2O$ was added to the dissolver solution; the slurry was stirred at 94°C for 1 hour; 7.8 g. of $Ba(NO_3)_2$ was added to the slurry; the resulting slurry was stirred for 1 hour at 94°C.

(d) 7.2 g. of BaF_2 and 10.8 g. of $Ba(NO_3)_2$ were added to 50 ml of dissolver solution; the slurry was stirred at 94°C for 2 hours.

(e) 10.88 g. of BaF_2 and 5.4 g. of $Ba(NO_3)_2$ were added to 50 ml of dissolver solution; the slurry was stirred at 94°C for 2 hours.

(f) This dissclver solution had 1.7M Zr, 1.8N H^+, and a F - Zr mole ratio of 5 to 1.

(g) This dissclver solution had 1.6M Zr, 0.9N H^+, and a F - Zr mole ratio of 4.5 to 1.

Precipitation with Solid Barium Fluoride-Barium Nitrate or Solid Barium Hydroxide-Barium Nitrate

During the precipitation of barium fluozirconate from STR dissolver solution using either solid barium fluoride-barium nitrate or solid barium hydroxide-barium nitrate as the precipitants, Sr^{89-90} and Ce^{144} were carried almost quantitatively with the precipitate, about 20 per cent of the Cs^{137} present was carried, less than one per cent of the ruthenium was found in the precipitate, and about 0.3 per cent of the uranium was lost to the precipitate. Since the flowsheets proposed by Paige[4] recover all zirconium from wash solutions, a zirconium removal of about 94 per cent (precipitate plus wash solution, as shown in Table 2) was realized.

Barium hydroxide was substituted for other weak bases used by Paige[4], in combination with barium nitrate, to supply barium for the precipitation as well as neutralize excess acid. Low acidity favors high zirconium recovery.

The use of barium fluoride in combination with barium nitrate permits adjustment of the fluoride-zirconium mole ratio without acid addition. No difference in fission product behavior, uranium loss, or zirconium recovery was indicated when barium fluoride-barium nitrate was used to precipitate barium fluozirconate from STR dissolver solutions ranging in acidity from 0.9N to 1.7N. X-ray examination of a barium fluozirconate precipitate formed using barium fluoride-barium nitrate as the precipitant showed the precipitate to be identical to those prepared previously[4], and believed to have a 6 to 1 fluoride to zirconium mole ratio.

Precipitation with Solid Barium Nitrate

Precipitation of barium fluozirconate using solid barium nitrate only, without the addition of barium fluoride or barium hydroxide, resulted in less Ce^{144} and Sr^{89-90} being carried on the precipitate, lower zirconium removal from STR process solutions, and higher uranium losses to the precipitate. The latter two effects were more marked when the acidity and fluoride concentration of the STR dissolver solutions were increased. X-ray examination of barium fluozirconate precipitated from STR solutions of both 3.3N acidity (having a fluoride to zirconium mole ratio of 6 to 1) and 1.7N acidity (having a fluoride to zirconium mole ratio of 5 to 1) showed the precipitates to be identical to a slow forming, structurally unidentified, precipitate sometimes found in previous work[4] when making a barium fluozirconate precipitation using solid barium nitrate as the only precipitant. Thus, in the work summarized in Table 2, experiments involving use of solid barium nitrate were probably terminated before the precipitation reaction had been completed. Differences between precipitations carried out utilizing solid barium nitrate alone as the precipitant and those using either solid barium fluoride or barium hydroxide in addition could possibly be eliminated by carrying out the former precipitation reaction for a longer period of time, using more efficient stirring during the precipitation, or adding barium nitrate as a solution.

2. Corrosion of Potential Evaporator Materials in the Barium Fluozirconate Process: N. D. Stolica, Problem Leader; M. R. Bomar

In the evaluation of materials of construction for evaporators in the barium fluozirconate process, several stainless steels were tested in evaporator product solutions at 95°C. The solutions were 4M nitric acid-0.1M barium fluozirconate and 1M nitric acid-0.1M barium fluozirconate-0.4M barium fluoride[4]. Corrosion rates for the fifteen-day test period are shown in Table 3.

TABLE 3

CORROSION IN BARIUM FLUOZIRCONATE PROCESS EVAPORATOR SOLUTIONS AT 95°C

Material	Corrosion Rate (mils per month) in 4M HNO_3-0.1M $BaZrF_6$	in 1M HNO_3-0.1M $BaZrF_6$-0.4M BaF_2
Carpenter 20	7.1- 6.6	5.1- 5.2
Carpenter 20 (welded)	14 -10	5.4- 6.4
SS 347	9.5- 9.2	8.0- 8.0
SS 347 (welded)	14 -14	9.2- 6.9
SS 304L	12	7.4-11
SS 304L (welded)	9	8.0- 6.1

Both Carpenter-20 and type 347 stainless steel showed severe intergranular attack and preferential weld attack. Although the rates are higher than desirable, the use of nominal amounts of aluminum nitrate to complex any remaining fluoride may lead to a usable flowsheet and material of construction.

B. Aqueous Ceramic Fuel Reprocessing

1. Chemical Reprocessing of BeO-UO_2; J. W. Codding, Problem Leader; L. A. Decker

Preliminary studies of the molten ammonium bifluoride (MAB) treatment for the recovery of uranium from spent ceramic fuels containing beryllium oxide have been completed. An earlier proposal[7] for reprocessing such fuels involved dissolution in MAB followed by recovery of uranium by fluoride volatility. The data reported here represent studies of an alternate method of uranium recovery by aqueous reprocessing.

Beryllium Oxide Dissolution

Initial dissolution rates of several refractory oxides and metals have been determined. The experimental methods and most of the results have been reported previously[5]. An extension of this study shows that

the dissolution rates of beryllium oxide in MAB at 135° and 165°C are 0.075 and 0.17 mg/(cm^2)(min), respectively. These rates may be compared with previously reported rates of 0.23 and 1.7 mg/(cm^2)(min) at 195°C and 227°C, respectively. A plot of Log Rate vs 1/T gives (from the Arrhenius equation) an activation energy of 3.78 Kcal/mole for the dissolution of beryllium oxide in ammonium bifluoride. In arriving at this figure, the rates observed at the boiling point (227°C) were neglected since erosion as well as dissolution affected the rate of weight loss.

Uranium Oxide Solubility

An indication of apparent uranium oxide solubility in MAB was obtained by filtering a "solution" of uranium oxide in MAB through a 20 micron sintered stainless steel filter. Essentially no uranium was retained on the filter; uranium concentration in the filtrate was 21 grams/liter. The filtrate was readily dissolved in nitric acid yielding an aqueous solution containing 20 grams/liter of uranium.

To determine whether a true solution of uranium in MAB had been formed, a sample of about 30 ml of MAB containing 0.818 grams of uranium was cooled, without agitation, from 227°C to 140°C over a period of 35 minutes, then quenched in air to room temperature. The test tube containing the solidified sample was then broken into three, approximately equal, portions. Each portion was dissolved in nitric acid and analyzed for uranium. It was found that 51.8 per cent of the total uranium had settled, during cooling, to the bottom third of the tube; 28.5 per cent remained in the middle portion, and only 19.7 per cent remained in the top section. Such stratification indicates that a true solution of uranium in MAB had not been achieved. The apparent particulate nature of the uranium in the molten phase should not cause much process difficulty, however; in one flowsheet the uranium would be continuously removed as the volatile fluoride, and in the other the salt phase would be immediately converted to a nitric acid solution. In either case, it appears that the concentrations of uranium attainable in the molten salt and aqueous systems are sufficiently high to provide a practicable process.

C. General Aqueous Studies

1. Solvent Stability Studies: E. M. Vander Wall, Problem Leader; A. J. Moffat

The effect of extracted zirconium and nitric acid upon the chemical stability of diluent-free tributyl phosphate (TBP) was investigated using gas-liquid chromatography for qualitative and quantitative analysis of the volatile products. The results of the study to date are being summarized in a report now in preparation(6).

The pertinent conclusions are as follows:

a. The TBP-HNO_3 reaction was found to be a dealkylation reaction with n-butyl nitrate as the major volatile product over the organic-nitric acid concentration range studied.

b. Extracted zirconium was found to degrade TBP approximately one thousand times faster than extracted HNO_3.

c. The major products of the TBP-Zr reaction were found to be n-butyl nitrate and $Zr(NO_3)_2(DBP)_2$.

d. Solid $ZrONO_3 \cdot 2H_2O$ (or $ZrOCl_2 \cdot 8H_2O$) was found to degrade TBP very rapidly with the production of amorphous zirconium organic phosphates and n-butyl nitrate (or chloride).

2. Evaporation and Mixing in a Packed Evaporator:
J. A. Buckham, Problem Leader; G. K. Cederberg

The results of evaporation tests and additional mixing tests which complement last quarter's mixing test results[5] are presented. This work concludes the studies of the performance of an evaporator packed with Raschig rings to simulate a possible means of criticality control in a non-geometrically safe vessel through uniform interior distribution of neutron absorbing materials.

Evaporation Studies

Evaporation tests in the 30-inch diameter packed evaporator, used in the mixing tests previously described[5], showed that the evaporation rates were comparable to rates in the unpacked evaporator and that operation was satisfactory although boil-over occurred more readily. The more tortuous paths for the vapor through the packing evidently caused the body of liquid to be expanded. Boil-overs were prevented by using lower liquid levels, lower pressure steam, and a small stream of sparge air to induce circulation and prevent local superheating during startup. No significant concentration gradients were induced by the packing during normal operation.

The evaporation rates were measured while using the bottom- and side-heating jackets together at various steam pressures between 30 and 90 psig for the three conditions: no packing, 1 1/2-inch Raschig ring packing, and 1/2-inch Raschig ring packing. The overall heat transfer coefficients (U_o) obtained are plotted in Figure 3 against the prevailing overall temperature difference between the steam and the solution (Δt_o). No statistically significant difference was evident between heat transfer coefficients obtained with either packing or without packing.

Neither solution type (water or aluminum nitrate) nor air-sparging had a statistically significant effect on the heat transfer rate. Therefore, the data were pooled and, by a regression analysis, an equation of the form $U_o = a(\Delta t_o)^{n-1}$ (where a and n are constants for each individual case) was derived and is indicated on Figure 3.

A series of tests was also made to evaluate the effect on the heat transfer rate of using the side-heating jacket alone, while using the two sizes of Raschig ring packing. However, because the side jacket represented 81 per cent of the total jacket area, the best-fit equation

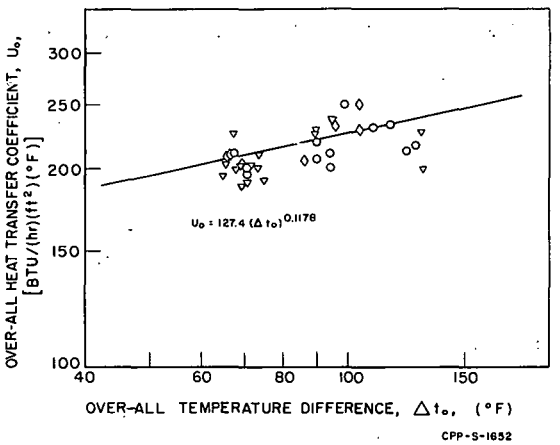

Fig. 3 - Evaporator Heat Transfer Coefficient Using Both Side and Bottom Jackets

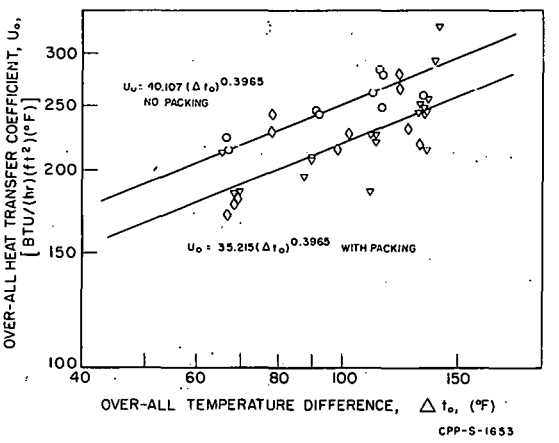

Fig. 4 - Effect of Packing on Heat Transfer Coefficient Using Bottom Jacket Only

○ - No Packing
▽ - 1 1/2-inch Raschig Ring Packing
◇ - 1/2-inch Raschig Ring Packing

was not significantly different from the equation for the two-jacket data presented above.

A third series of evaporation tests was made using the bottom jacket alone, with water and aluminum nitrate, over the steam pressure range of 30 to 120 psig. These data are plotted in Figure 4. The regression analyses of these data and the tests for the significance of packing showed that the heat transfer coefficients obtained in the unpacked tank were slightly greater than those obtained when packings were used.

Mixing Induced by Addition of Liquid

Several tests of limited scope showed qualitatively the degree of mixing obtained by introducing one solution onto the top of another solution of dissimilar density. The cases studied were (1) the addition of water to quiescent aluminum nitrate (about 2M) for three vessel conditions: no packing, 1 1/2-inch Raschig ring packing, and 1/2-inch Raschig ring packing; and (2) the addition of aluminum nitrate to quiescent water for the same vessel conditions. For each test, approximately 40 gallons of the test liquid were added at a rate of 3 to 4 gpm to the base solution, initially at a depth of about 16 inches in the tank. The test solution entered through a one-inch nozzle in the top of the tank and either fell free into the tank without packing, or into the bed of packing (35 inches deep), with the drop decreasing from 30 inches to 15 inches in the course of the addition. Samples were taken immediately after completion of the addition.

Slight differences existed in the initial liquid level and in the initial concentrations, C_o, of the aluminum nitrate used in each test. To equalize the effect of these variations, the tests were compared on the basis of the concentration ratio of aluminum nitrate (final/initial) at

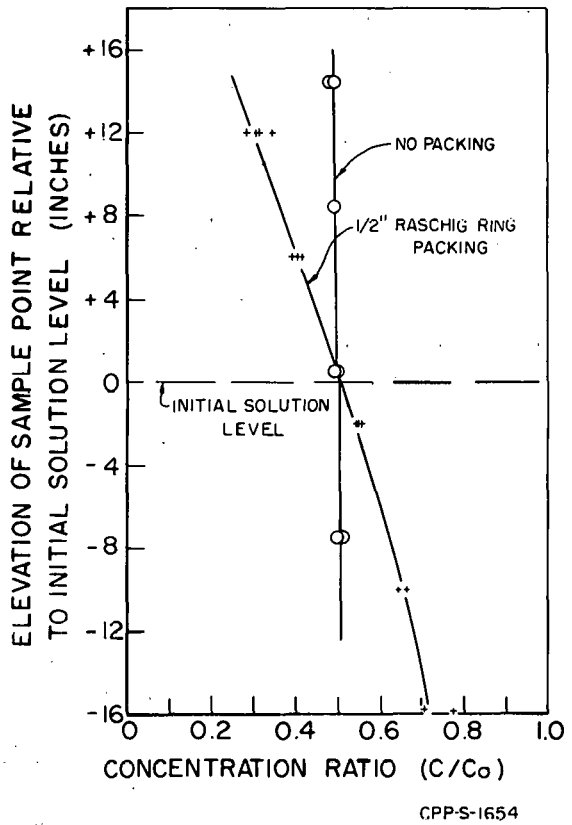

Fig. 5 - Mixing Induced by Adding Concentrated Aluminum Nitrate (Relative Concentration 1.0) to Water

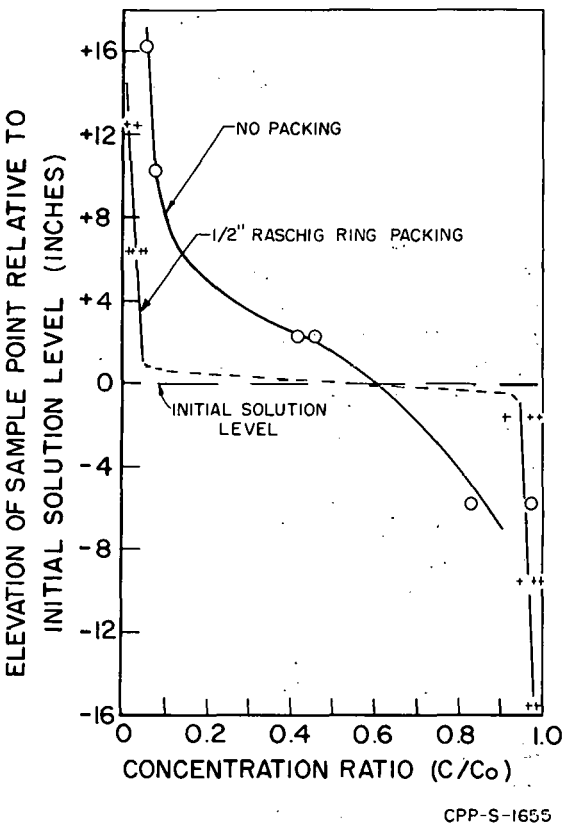

Fig. 6 - Mixing Induced by Adding Water to Concentrated Aluminum Nitrate

several levels above and below the starting level in the tank as illustrated in Figures 5 and 6. These show the concentration variations with level at the completion of the combination of the two liquids in each experiment.

Figure 5 shows that immediately after aluminum nitrate was added to water in the unpacked tank the aluminum nitrate concentration was nearly uniform throughout the vessel, without air sparging. It also shows that when the 1/2-inch packing was used the aluminum nitrate was less completely mixed as it descended to the bottom.

Figure 6 shows that when water was added to the aluminum nitrate in the tank it tended to remain on top of the aluminum nitrate. When there was no packing in the tank the concentration varied continuously from bottom to top with a more abrupt change at the mid-point. However, when the tank contained the 1/2-inch Raschig rings, there was very little concentration change in the bottom half of the vessel and a very abrupt concentration change at the original top elevation of the aluminum nitrate.

IV. WASTE CALCINATION DEVELOPMENT AND DEMONSTRATION

Section Chiefs: J. A. Buckham, Technical Projects
D. W. Rhodes, Waste Treatment
K. L. Rohde, Process Chemistry
J. I. Stevens, Waste Calcination Demonstration

Laboratory and pilot plant studies on the fluid bed calcination technique for reduction of aqueous aluminum nitrate waste solutions to solid alumina form have continued. The pilot plant two-foot square calciner was operated, using a nozzle intended for installation in the Demonstrational Waste Calcining Facility, to gather data directly applicable to the demonstrational unit on operable liquid feed rates and nozzle air-to-liquid feed ratios as well as information on the attrition rate of the product during fluidization as affected by nozzle atomizing air rates, fluid feed rate, and fluidizing air rate. Erosion of the nozzle observed during these tests led to the study of nozzle designs and development of an extended cone tip, less susceptible to wear by impingement of alumina particles under the influence of an air vortex.

A method of determining calcine particle density and intra-particle porosity has been developed for use in certain theoretical calculations.

The physical structure of the alumina produced during operation of the fluidized bed calciner has, for unknown reasons, rapidly shifted between an amorphous and a predominantly alpha crystalline form. Results of examination of bulk product produced in the pilot plant, fines carried in the off gas, and dissected particles are discussed in terms of a possible sequence of events leading to the observed condition. A basic laboratory investigation of the calcination reaction has been initiated in an effort to understand the controlling factors in the process, the first approach being study of the simple kinetics of conversion of amorphous alumina to various crystalline forms of alumina. Factors under consideration are time, temperature, concentration of minor components such as sodium nitrate and mercury, and composition of the atmosphere in the calciner. Amorphous alumina has been converted to an extent of approximately 65 per cent to crystalline alumina, as measured by X-ray analysis.

Laboratory corrosion tests on the materials of construction were verified by a recent inspection of the two-foot square calciner after prolonged pilot plant service. The choice of Carpenter 20 for the calciner body, stainless steel Type 316 for the NaK heater and Carpenter 20 for the fluid bed heat exchanger was shown to be satisfactory by field measurements.

The calcination of fluoride-containing wastes from the processing of zirconium-uranium fuels poses a serious problem in materials of construction if hydrofluoric acid is liberated. The addition of CaO to such wastes has shown promise of fixing 99 per cent of the fluoride in the solid product. Detailed experiments are described in which fluoride volatility is related to stoichiometry of added CaO, temperature of calcination, zirconium-aluminum concentration, and nitrate concentration. The leachability of the calcine was also correlated with the method of preparation.

The Demonstrational Waste Calcining Facility was not completed during this period as scheduled; present status is estimated at 98 per cent complete.

A. Research and Development in the Pilot Plant

1. Studies in the Two-Foot Square Calciner Unit:
E. S. Grimmett, Problem Leader; B. R. Wheeler

A performance study of a nozzle intended for use in the Demonstrational Waste Calcining Facility (DWCF) was made in the two-foot square calciner; the nozzle performance was satisfactory from a process standpoint. For this study, the only difference from the pilot unit equipment previously described[8] was the substitution of a single Spraying Systems Company type 1/2 J feed nozzle for the two pairs of opposed, smaller, feed nozzles. Data were obtained on attrition effects, temperature effects, operable nozzle air-to-liquid volume ratios, operable feed rates, and physical characteristics of the calciner product.

Attrition Effects

Preliminary to the calcination study with the nozzle, the factors affecting attrition rate during fluidization were partially isolated. A direct measure of the change in product size with time would be the best method of determining attrition rate; however, such a procedure would have been burdensome for this scoping study. The simple direct method of measuring the quantity of fines per hour leaving the calciner vessel via the off gas, i.e., bed depletion rate, was chosen as a relative index of the product attrition rate. Bed depletion rate, of course, does not uniquely reflect product attrition rate because the size (and hence quantity) of alumina elutriated from the calciner is also a function of the superficial fluidizing gas velocity. For example, an increase in the fluidizing gas velocity from 0.8 ft/sec to 1.35 ft/sec will result in a corresponding change in the upper size limit of elutriated particles from 120 to 160 microns. Therefore, both elutriation and attrition effects are necessarily confounded in the measurements made. More refined measurements were not considered necessary at this time as the indices obtained do give the desired semi-quantitative indication of the relative amounts of attrition caused by the important variables in fluidized bed calcination.

The quantity of fines leaving the calciner vessel per hour via the off gas was determined at two fluidizing velocities and two nozzle air rates, with and without water feed. In addition, this index was noted without either nozzle air or water feed at two fluidizing velocities. These tests were conducted at a normal calcining temperature, 500°C, and the data were collected after thermal equilibrium in each case. The results of these tests show that:

(a) The quantity of high-velocity nozzle atomizing air has (through a jet grinding action) a significant effect on product attrition which in turn affects bed depletion rate. For example, when

atomizing air (but no liquid) was introduced through the feed nozzle into the fluidized bed, the rate of bed depletion increased tenfold, to over 7000 grams per hour. In this case the atomizing air rate was only about 12 per cent of the fluidizing gas and was equal to that amount required to maintain an air-to-liquid volume ratio of 500 if the liquid rate were 80 liters per hour. A further increase in the atomizing air rate, to the equivalent of an air-to-liquid ratio of 880, was accompanied by a significant increase in the rate of bed depletion.

(b) When water feed at the rate of 80 liters per hour was introduced at either of these nozzle air rates, there was an almost 100 per cent increase in rate of bed depletion. This higher weight loss may have been partially caused by the increased space velocity of the total fluidizing gas. (Addition of the water feed increased the superficial velocity of the fluidizing gas at the top of the calciner from 0.8 ft/sec to 1.35 ft/sec.) A second cause of the increased bed depletion rate could be a higher product attrition rate presumably caused by thermal shock of the water feed contacting the hot calcine product.

(c) During the calcination of aluminum nitrate solution, the attrition effect of the nozzle air on the bed material was lessened (as has been repeatedly noted in earlier work), perhaps because the bed particles were being continuously coated with new material or perhaps because of occlusion of fines in the liquid spray and subsequent deposition on larger particles.

(d) The superficial velocity of the fluidizing gas had a much smaller effect on rate of bed depletion in the limited area studied than did the nozzle air or the introduction of water feed. A change in inlet superficial velocity from 0.8 to about 1.1 feet per second caused an approximately 20 per cent increase in the rate of bed depletion, i.e., to more than 9000 grams per hour during a period when nozzle air but no liquid was fed. The increased depletion rate was probably due primarily to increased elutriation rather than increased attrition.

Temperature Effects

A temperature traverse in the spray nozzle zone during the attrition test, along with numerous temperatures from thermocouples placed throughout the bed, indicated that no extensive temperature depression was caused by a water feed rate of 80 liters per hour through the one nozzle. The results show that beyond a distance of 12 to 15 inches from the nozzle along the axial centerline, normal bed temperature was attained. Subsequent traverses during periods with aluminum nitrate feed rates of 80 and 120 liters per hour, at nozzle air-to-liquid volume ratios of 640 and 300, respectively, also exhibited similar temperature profiles.

Operating Rates and Nozzle Ratios

The first calcining test with the DWCF nozzle was made to determine whether a feed rate of 80 liters per hour could be put through a single nozzle without caking the bed, since there must be an upper limit to the quantity of feed which can be concentrated into a narrow

zone and yet achieve sufficient heat transfer to maintain satisfactory calcination.

Calcining conditions for this test (No.11) along with those of a later run (No.12) are given in Table 4.

TABLE 4

OPERATING CONDITIONS FOR TEST OF DEMONSTRATIONAL WASTE CALCINER FACILITY NOZZLE IN TWO-FOOT CALCINER

	Run No.11	Run No.12
Temperature, °C	500	400
Feed Rate, liters/hr	80	120
Superficial Velocity of Fluidizing Gas, ft/sec	0.78	0.90
Nozzle Air-to-Liquid Volume Ratio (Reduced stepwise within range shown for Run No. 1)	590 to 120	300
Bed Pressure, psia	18.5	20
Fines Recycle	None	None
Feed Composition:		
Aluminum nitrate, M	1.95	1.29
Nitric acid, M	1.25	2.84
Sodium nitrate, M	0.089	0.078
Mercuric nitrate, M	0.006	0.015

Starting at the nozzle air-to-liquid volume ratio of 590 (which was later reduced to 500), the calciner was successfully brought to an essentially steady-state condition. Only minor fluctuations in product characteristics were still apparent on the eighth day when a forthcoming power outage prompted a decision to establish the lower operable limit of the nozzle air requirements prior to designing the subsequent run program. During the final three days of operation the nozzle air-to-liquid volume ratio was reduced stepwise in increments of 50, at 16-hour intervals, until this action had resulted in an increase in the mean product particle diameter to 1.0 mm (as compared with the steady-state diameter of 0.4 mm) at which point poor heat transfer from the NaK tubes to the bed required run termination. (The last nozzle ratio used was 120.) Subsequent examination of the alumina bed showed no evidence of caking; the lower operable limit of the nozzle ratio (which governs the mean spray droplet size) has, therefore, not yet been established. The product characteristics from both the steady-state period and the final period of operation are given in Table 5.

TABLE 5

PRODUCT CHARACTERISTICS FROM DWCF NOZZLE RUN NO. 11

	Steady-State	Final
Bulk Density, g/cc	0.67 - 0.71	0.71
Mass Median Particle Diameter, mm	0.4	1.0
Product rate, kg/hr	7.7	5.4 - 7.3
Crushing strength index[5], grams	130 - 150	350 - 450
Alpha Alumina, percentage	12 - 14	7 - 8
Nitrate Content, millimoles/gram	0.75 - 0.79	0.9
Absolute Material Density, g/cc	2.82 - 2.85	2.75

The encouraging results of the first study prompted a run with a feed rate of 120 l/hr to establish if a higher volume of liquid feed could be concentrated into a narrow spray zone without caking the bed. The run conditions are given in Table 4, run No.12. The calcining temperature was lowered to 400°C at the 120 l/hr feed rate because the DWCF may operate at this temperature. Blower and compressor limitations established the fluidizing gas velocity and the nozzle air rate used on this run. The feed composition during this portion of the nozzle study was adjusted to the specifications of the feed (with scrub recycle) which will be processed in the DWCF.

This run (No. 12) lasted 8 days and was again terminated when excessive bed particle growth resulted in poor heat transfer from the NaK tubes to the bed. Examination of the final bed revealed no evidence of product caking. It may be concluded from this scoping study that feed rates of at least 120 l/hr can be put through a single nozzle into a fluidized bed calciner (the DWCF design flowsheet value is 150 l/hr per nozzle); however, a more effective means of controlling product particle size must be employed. This could be done by using higher nozzle air-to-liquid ratios, by returning fines to the bed (as will be done in the DWCF), or by introducing a high velocity attrition air stream into the bed.

The obvious difference in product characteristic between the two runs was a change in the bulk density from 0.71 g/cc[5] in the first run to a high of 1.18 g/cc (which finally declined to 0.9 g/cc) in the second run. Accompanying this differing bulk density was a steadily decreasing alpha alumina content to a low of 2 per cent at termination of the second run. This was the first occasion on which the desirable combination, high bulk density and low alpha content, has been observed. Additional studies will be made to determine the range of operating conditions under which this combination can be achieved.

2. Calcine Particle Density

A method of determining the apparent particle density of calcine product has been developed by the ICPP Analytical Development Group. This method, patterned after one described in an article by Beirne and Hutcheon[9], is based on a mercury displacement technique. Briefly, the method consists

of drawing a high vacuum on a product sample to expel air, introducing mercury, and then applying pressure to force the mercury around the individual particles. The high surface tension of the mercury is assumed to prevent particle penetration; however, the validity of this assumption will depend on the pore size of the particles. Lack of a satisfactory standard with known particle density prevents an estimate of analytical error for calcine particle density; however, Beirne and Hutcheon indicate a precision of $\pm$ 0.01 g/cc for coke particles. The method has been used to determine the particle density of calcine product from various runs. The bulk density is 59 per cent of the particle density in the same units of measure. This means that funnel-poured alumina from fluidized bed calcination, over the particle size ranges encountered in these studies, has a constant inter-particle void fraction of 0.41.

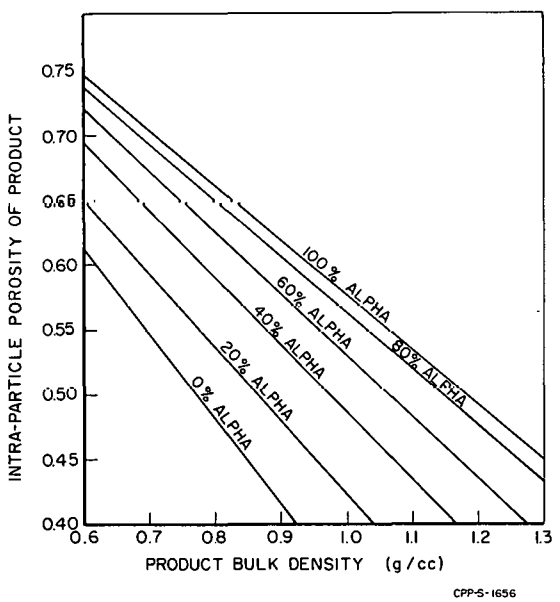

Fig. 7 - Intra-Particle Porosity of Alumina Product From Two-Foot Square Calciner

The particle density has long been sought in these studies because it is a required factor in elutriation calculations and in certain other mathematical relationships. The knowledge of particle density together with with the absolute density of calcine product[5] has also made possible the calculation of intra-particle porosity, a basic property of the alumina not heretofore known. Figure 7 shows the calculated relationship between intra-particle porosity and the bulk density of the alumina with alpha alumina content as a parameter. The curves were developed from the previously published[5] relationship between alpha alumina content and product absolute density and the above mentioned finding that bulk density is 59 per cent of the particle density.

3. Alpha Alumina Product and Off Gas Loading

The physical structure of the alumina produced during operation of the fluidized bed calciner has, for unknown reasons, rapidly shifted between an amorphous and a predominantly alpha structure[5]. The alpha content of the product affects particle size, off gas loadings, and the bulk density of the product.

During periods when the alumina in the calciner bed was predominantly (over 60 per cent) alpha, the off gas loading has been excessive, indicating that a high rate of product attrition was occurring. The rate of fines leaving the calciner vessel along with the off gas is shown as a function of the alpha alumina content of the product in Figure 8. Product entrainment by the fluidizing gas has elutriated more than 50 per cent of the alumina product, via the off gas, when the alpha alumina content of the product exceeded 70 per cent.

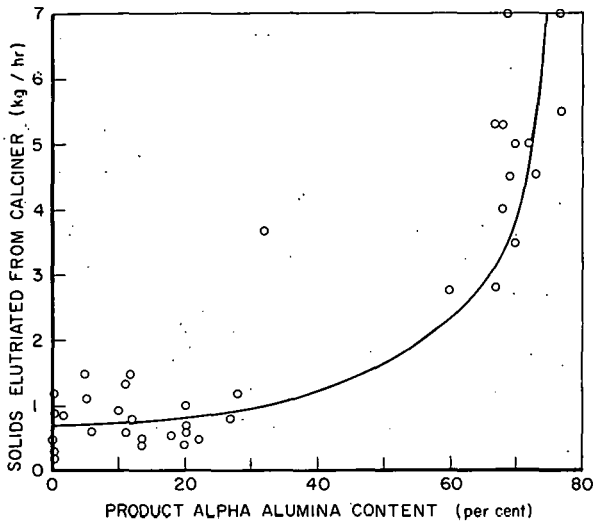

Fig. 8 - Off Gas Loading for Two-Foot Square Calciner. (Calciner feed rate, 8.6 kg/hr, based on solids content; no recycle of fines)

Data have been collected to study the attrition mechanism and to seek the cause for an amorphous bed suddenly shifting to the crystalline structure, resulting in the excessive gas loadings and vastly different product properties. Pertinent data are given in Table 6.

The samples from May 8 to June 1 were taken from one continuous run. The data show that a large increase in the bulk product alpha alumina content took place during the twenty-four hour period between May 21 and 22. To elucidate the manner in which this change took place, individual particles were removed from each day's sample, cut in half, and portions taken from the cores and the skins. These portions were analyzed for alpha alumina; results are reported in the third and fourth columns of Table 6. These results show that during the period May 8 to 21 the cores of the particles had a higher alpha alumina content than either the bulk product or the outer skins. However on May 22, the alpha content of the skins became equal to the alpha content of the cores and continued equal for the remainder of the run.

TABLE 6

ALPHA ALUMINA CONTENT OF PRODUCT FRACTIONS
(Per Cent Alpha Alumina)

Date of Sample	Bulk Product	Product Particle Cores*	Product Particle Skins*	Off Gas Fines
May 8	6	20	< 20	--
May 12	20	50	< 20	--
May 17	20	40	< 20	10
May 21	28	40	24	22
May 22	60	45	45	--
May 23	63	58	58	46
May 30	72	60	60	43
June 1	68	--	--	40

*The necessarily small sample size (about 50 individual particles constituted a sample) caused difficulty in establishing accurate values, so minor differences should not be regarded as significant.

The data also show that the solid material elutriated from the calciner into the off gas had, in every case, an alpha alumina content which was lower than that of the bulk product or of the cores or skins of the individual particles.

The reason for the sudden transition in the alpha alumina content of the product is not apparent from these data. Some conclusions as to the sequence of events leading up to this transition are possible, but the exact triggering mechanism is unknown. It is apparent that when the bed is essentially amorphous alumina the freshly-formed layer on a particle is also largely amorphous. This is indicated both by the particle skin composition and the alpha content of the off gas fines. Further, it appears that the spray-dried material from the nozzle has a very low alpha alumina content since the off gas fines always have a lower alpha content than the skins of the particles. (It is believed that the off gas fines are created both by attrition of the bed particles and by direct spray-drying of atomized droplets. Hence the alpha alumina content of the off gas fines should reflect the alpha alumina content of both the particle skins and the spray-dried material.)

After the bed had changed to a product with a high alpha alumina content (May 22 to June 1) the inside and outside of the particles had a similar alpha content. At this point the off gas fines had increased considerably in alpha content, but they still contained a significantly lower concentration of alpha alumina than the particle skins. It would thus appear that even though the layer being applied to a particle was initially amorphous alumina, conditions were such that a very rapid conversion to the alpha phase occurred.

In any event, it is clear that the alpha alumina content of calcined material is important for process control reasons; current emphasis is being given the further elucidation of the mechanism of formation of alpha alumina.

4. Twelve-Inch Calciner Design

Modification of design drawings for the 12-inch calciner[5] is continuing. Completion of the drawings in the near future will permit resumption of construction. The 12-inch calciner system is designed for flexibility and will permit extensive development studies not possible in the existing two-foot square calciner.

B. Laboratory Investigations

1. Calcination of Aluminum Nitrate Wastes:
D. W. Rhodes, Problem Leader; R. F. Murray

Preliminary scoping studies were made in search of factors influencing the formation of amorphous vs crystalline alumina when aluminum nitrate is converted to aluminum oxide in a fluidized bed calciner. The nature of the alumina formed has significant effects on calciner operation and physical properties of the product[5].

The primary objective of the laboratory research was to determine what factors influence the formation of alpha alumina, but not necessarily to establish the degree to which these factors affect the formation of this crystalline compound. Preliminary laboratory research resulted in converting amorphous calcined alumina to an extent of approximately 75 per cent to crystalline alumina (~45% γ and 30% α) at 500°C. Possible factors, which appear to be important in this phase transformation, include time, temperature, concentration of $NaNO_3$, and composition of the calciner atmosphere.

Experimental Methods and Equipment

A reaction chamber was developed for treating samples of alumina at various temperatures in a continuous stream of nitric acid vapors (Fig. 9). The HNO_3 vapors were obtained by dropping HNO_3 solution into the heated chamber where it was picked up by the heated air stream and passed through the samples.

The initial scoping experiments consisted of heating samples of amorphous alumina and aluminum nitrate in air and in an atmosphere containing HNO_3 vapors, both with and without added chemical impurities, in an attempt to effect a phase transition from amorphous to alpha alumina at a temperature of 500°C. Microscopic examination of samples of calcined alumina and determination of hardness across the cross section of individual particles, by use of a microhardness tester, were also attempted.

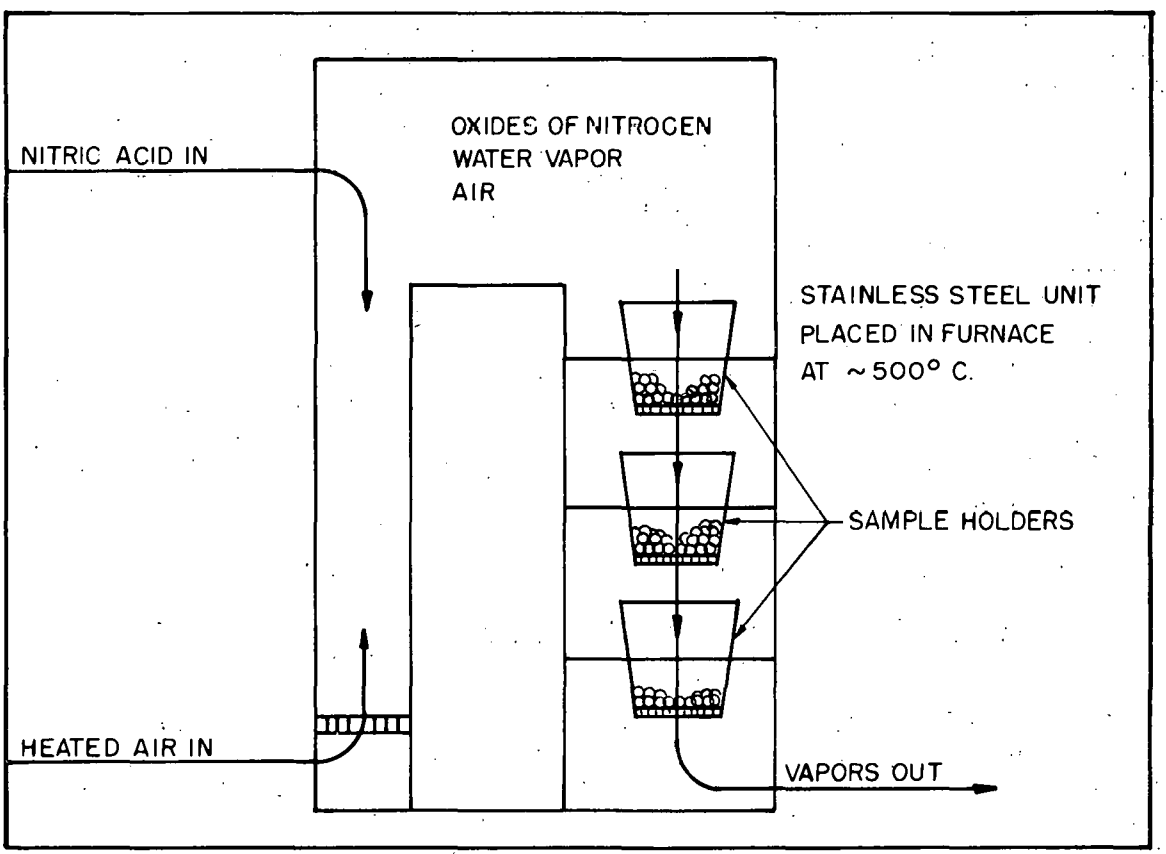

Fig. 9 - Equipment for Studying Phase Changes in Calcined Aluminum Nitrate Waste

Experimental Results

The friability and layered characteristics of the calcined alumina specimens prevented a successful evaluation of the hardness characteristics across an individual particle. No additional attempts will be made to measure this property.

Mounting and polishing of the alumina specimens for microscopic examination was accomplished by use of a cold-setting plastic. This minimized the breakage which occurred when techniques involving a temperature change were tried. Even after polishing, the surface roughness was of such a magnitude that magnification greater than 100 diameters was impractical. All the specimens examined showed structural similarities, i.e., build-up of concentric layers and cross sectional cracking. A photograph of a typical specimen is shown in Figure 10.

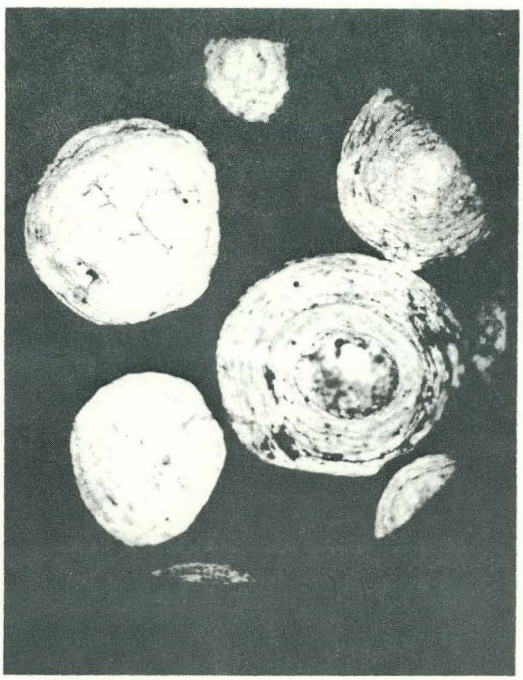

Fig. 10 - Photomicrograph of Alumina from Two-Foot Calciner - 3/26/60 - 25X
(90% alpha alumina; Hg and Na in feed)

The results of the preliminary scoping studies are summarized in Table 7. Examination of the data obtained by heating amorphous alumina in air indicated that at 800°C a trace (>5%) of alpha alumina formed, and at 927°C 60 per cent alpha alumina was produced after heating for nearly 200 hours. Appreciable amounts of gamma alumina were present in the samples at both temperatures. Some gamma alumina was formed at 500°C but no alpha alumina.

A sample of amorphous alumina containing about 4 wt. per cent $NaNO_3$ and heated for about 90 hours in nitric acid vapors produced 20 to 30 per cent gamma alumina and about 5 per cent alpha alumina at 450°C. Another sample of amorphous alumina containing 10 wt. per cent $NaNO_3$ was converted to 40 to 50 per cent gamma alumina and about 30 per cent alpha alumina after heating for about 90 hours. A similar experiment in which the concentration of nitric acid vapors was reduced by one-half produced only a small amount of gamma alumina and no alpha alumina.

Although these data represent only single experiments and have not been duplicated, they do point to variables which appear to be important in the transition from amorphous to alpha alumina. For example, time, temperature, concentration of HNO_3 vapors and concentration of $NaNO_3$ all appear to be important in the formation of alumina. These variables will be studied in detail. In addition, the presence of $Hg(NO_3)_2$ will be investigated because of the presence of significant quantities of this chemical in the waste solutions.

TABLE 7

SUMMARY OF EXPERIMENTS ON FORMATION OF CRYSTALLINE ALUMINA FROM AMORPHOUS ALUMINA

Sample Number	Heating Time (hrs)	Temperature (°C)	Source of Calciner Atmosphere	Starting Material	Added Reagents	Product Composition		
						Amorphous (%)	Gamma (%)	Alpha (%)
1a	192	927	Air	A* Al_2O_3	----	15	25	60
4a	192	800	Air	A- Al_2O_3	----	45	50	< 5
6a	192	500	Air	A- Al_2O_3	----	75	25	none
7a	144	927	Air	A- Al_2O_3	0.14 g $NaNO_3$ per 5 g Al_2O_3	balance	small	65
8a	144	800	Air	A- Al_2O_3	0.14 g $NaNO_3$ per 5 g Al_2O_3	balance	high	< 5
9a	144	500	Air	A- Al_2O_3	0.14 g $NaNO_3$ per 5 g Al_2O_3	balance	low	none
10	66	500	6M HNO_3	A- Al_2O_3	----	balance	present	none
14	92	450	6M HNO_3	$Al(NO_3)_3 \cdot 9H_2O$	0.2 g $NaNO_3$ per 5 g ANN	100	none	none
15	92	450	6M HNO_3	A- Al_2O_3	0.2 g $NaNO_3$ per 5 g Al_2O_3	balance 0	20-30	5
20	70.5	500	2.8M HNO_3	A- Al_2O_3	0.5 g $NaNO_3$ per 5 g Al_2O_3	balance	small	none
23	70	500	2.8M HNO_3	A- Al_2O_3	0.2 g $HgCl_2$ per 2 g Al_2O_3	balance	small	none
25	90	500	6M HNO_3	A- Al_2O_3	0.2 g $NaNO_3$ per 2 g Al_2O_3	balance	40-50	30

* A = Amorphous Alumina

2. Service Test Corrosion Evaluation of the Two-Foot Square Calciner: N. D. Stolica, Problem Leader; T. L. Hoffman

Three important components of the two-foot square waste calciner have been inspected for corrosion damage after prolonged service. These were the direct fired stainless steel type 316 bundle in liquid metal service in the NaK heater, the Carpenter 20 calciner body, and the Carpenter 20 heat exchanger in the fluid bed. It was generally concluded that these materials were well chosen for these applications.

Direct Fired Liquid Metal Bundle

Liquid NaK (78 per cent potassium - 22 per cent sodium) is heated in a stainless steel type 316 bundle by an oil fired furnace. Stainless steel type 304 is used as a NaK transmission line to the 3/4" O.D. x 14 BWG Carpenter 20 fluidized bed heat transfer tubes. The furnace is fired by a 500,000 BTU/hr burner using ASTM D 396-48T Grade No. 2 oil. The upper temperature limit for the liquid metal is 1440°F (760°C). During the period June 1958 through June 1960, the furnace was operated at 1000-1440°F for about 5273 hours, and at 200-999°F for about 842 hours. During this period, about 115 starts were made.

An examination of the stainless steel type 316 liquid metal bundle with the unaided eye suggested that the alloy had suffered only minor corrosion damage. All tubes were coated with a porous, rather tenacious, non-uniform scale. Numerous pits, which were estimated to be less than 5 mils deep, were observed under the scale.

From micrometer measurements on one-half of the 35 vertical connecting tubes, a maximum of 17 mils loss was observed. This value represents about 2.3 mils per month loss during 5273 hours at above 1000°F or 2.0 mils per month loss during the total period of service. No evidence of preferential corrosion was found on either the top or bottom header tubes.

Fluidized Bed Heat Transfer Tubes

A tubular section was cut out of the Carpenter 20 (Cb) heat exchanger which had been in liquid NaK fluidized bed heat transfer service for 2206 hours at 1000°F-1440°F and 611 hours at 200°F-999°F. Tube dimensions, by micrometer measurement, were 0.750" O.D., 0.574" I.D., and 0.089" wall thickness. These dimensions are well within the limits of 3/4" O.D. x 14 BWG tubing. Accordingly, during the 2817 hours of operating time, corrosion associated with liquid NaK and the calcination product appears to be small.

Spot measurements of the outside diameter of the tubes after 6115 hours service were 0.745" $\pm$ 0.005". This represents a maximum loss to one side of the tube of 10 mils, i.e., a corrosion rate of 0.0012 inches per month.

Calciner Vessel Body

An inspection of the annealed Carpenter 20 vessel body indicated that it was passive to the calcination products and atmosphere.

3. Precipitation-Calcination of Fluoride Solutions:
R. L. Hickok, Problem Leader; J. S. Madachy

Work was continued from the previous quarter(5) on the precipitation-calcination of fluoride-containing solutions resembling zirconium process wastes. The waste solutions resulting from nearly any presently conceived aqueous process for zirconium-based reactor fuels are similar to that produced at the ICPP by the STR process. These are acidic solutions which contain, as major chemical components, zirconium, aluminum, fluoride and nitrate. The method under investigation for treating the solutions involves a precipitation step in which solid calcium oxide is used to neutralize the solution and precipitate the fluoride as calcium fluoride or zirconium and aluminum fluoride containing compounds. The resulting slurry is then calcined. The advantages of this method are (1) reduction of waste volume by conversion to a solid, and (2) containment of the fluoride as a stable salt, thus greatly reducing the corrosion hazard attendant to storage of acidic liquid wastes containing fluoride.

Method and Measurements

A simple laboratory procedure was developed to study the precipitation-calcination reaction. Samples (10 ml) of solution containing the desired concentrations of zirconium, aluminum, fluoride, and nitrate were prepared from stock solutions of zirconium nitrate, aluminum nitrate, hydrofluoric acid, and nitric acid. The solution was placed in a 50 ml platinum crucible, a weighed quantity of solid calcium oxide added, and the slurry stirred for two hours. The slurry was allowed to stand over night and then placed in the calciner vessel (Figure 11). The calciner temperature was gradually increased over a period of about two hours to a selected temperature, i.e., 300, 400, 500, or 600°C, and held at that temperature for four hours. At this time the heaters were turned off and the calciner cooled in an air stream.

During the entire calcination period air, from which carbon dioxide had been removed, was passed through the calciner and thence through a series of two caustic scrubbers (Figure 11). The rate of air flow was such that replacement in the calciner occurred three to four times per minute.

Following calcination, the solutions in the caustic bubblers were analyzed for fluoride content using a micro fluoride method developed by the ICPP Analytical Section. This is a spectrophotometric method in which the bleaching of the zirconium-eriochrome cyanine R color by fluoride is measured. The lower limit of the method is 5 μg of fluoride/ml.

The calcined solid was leached with water for 24 hours and samples of the solid were submitted for X-ray diffraction analysis. Some of the leachates were also analyzed for fluoride content.

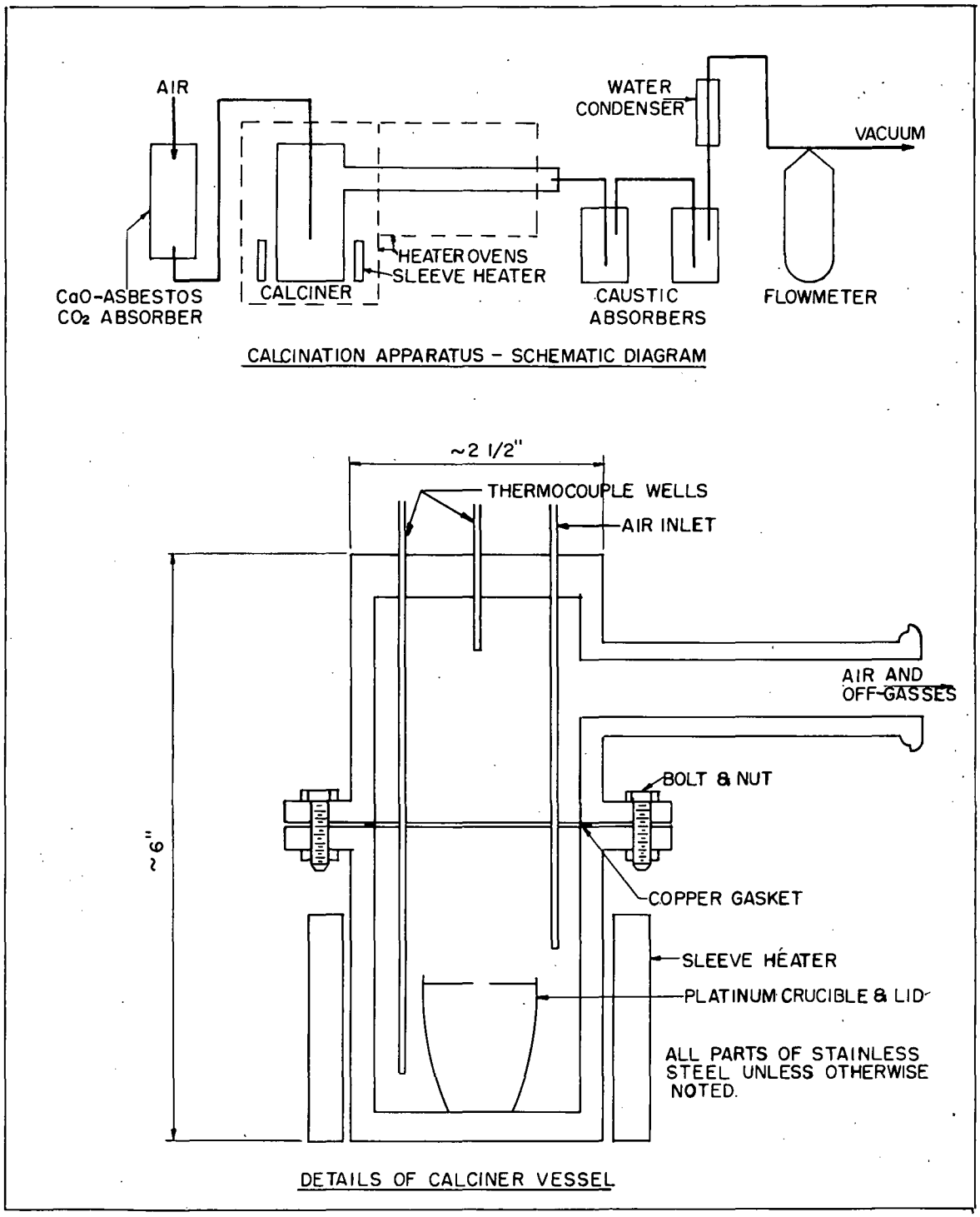

Fig. 11 - Calcination Equipment and Flow Diagram for Calcination of Zirconium Fluoride Wastes

Experimental Results

A series of 28 experiments completed the first phase of this program. In this phase an attempt was made to establish the effects of variation of reaction conditions on volatilization of fluoride during calcination and on leachability of the calcine. The reaction parameters studied included concentration of aluminum, fluoride and nitrate in the solution, the chemical equivalency ratio of calcium oxide to fluoride, and calcination temperature.

The results of these experiments are given in Figures 12 - 15. Figures 12 and 13 illustrate the effects of the CaO/F equivalency ratio and calcination temperature on fluoride volatility and calcine leachability, respectively. From these data it can be seen that low fluoride volatility was achieved by calcination at temperatures of 500°C or lower. The CaO/F equivalency ratio appears to have little effect on fluoride volatility if aluminum is present unless the calcination temperature was above 500°C. At 600°C, or in the absence of aluminum, however, an increase in the amount of calcium oxide added greatly repressed fluoride volatilization.

The per cent of calcine removed by leaching with water increased as the CaO/F equivalency ratio increased or as the calcination temperature decreased. The higher leachability at high (i.e., 1.5) CaO/F ratios was probably due to excess CaO in the calcine. Un-decomposed nitrates probably accounted for the greater solubility observed in calcines obtained at 300° and 400°C. At these lower temperatures the presence of calcium appeared to inhibit decomposition of nitrate. This is illustrated in Figure 14 in which the per cent nitrate decomposition is plotted as a function of the CaO/F equivalency ratio with all other parameters held constant.

The effect of nitrate concentration on fluoride volatilization is shown in Figure 15. This effect is not clearly understood on the basis of the present data, but it appears that a maximum fluoride volatility results at nitrate concentrations in the range of 2 to 3 M. Leachability of the calcine seems to be little affected by the nitrate concentration in the feed solution.

The effect of aluminum concentration on fluoride volatilization cannot be explained completely by the available data. It appears that aluminum repressed fluoride volatilization when the CaO/F ratio was less than 1, but had little effect when the ratio was 1 or greater.

Calcination temperature, as shown in Figures 12 and 13, affected both fluoride volatilization and product leachability. The volatilization of fluoride increased slightly as the temperature increased from 300 to 500°C but increased greatly at 600° unless the CaO/F equivalency ratio was 1.5 or, perhaps, higher. Calcine leachability was inversely related to calcination temperature as illustrated in Figure 13. This is apparently due to incomplete removal of nitrate as is shown in Figure 14.

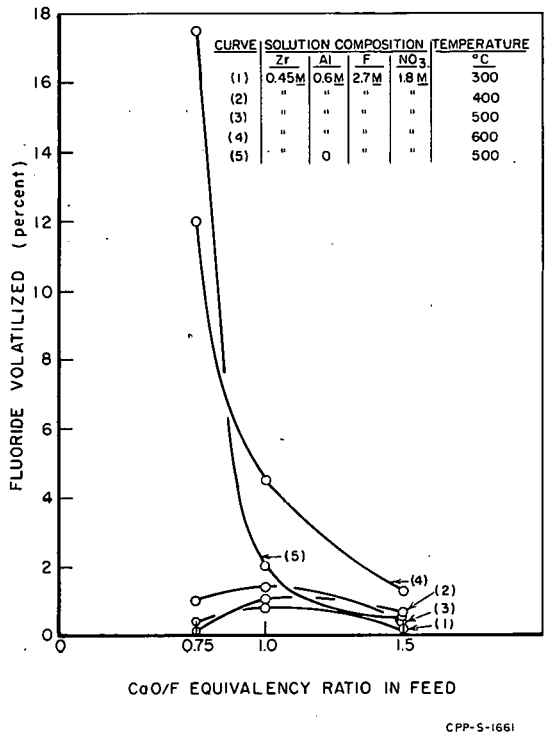

Fig. 12 - Effect of Calcination Temperature and CaO/F Equivalency Ratio on Fluoride Volatility

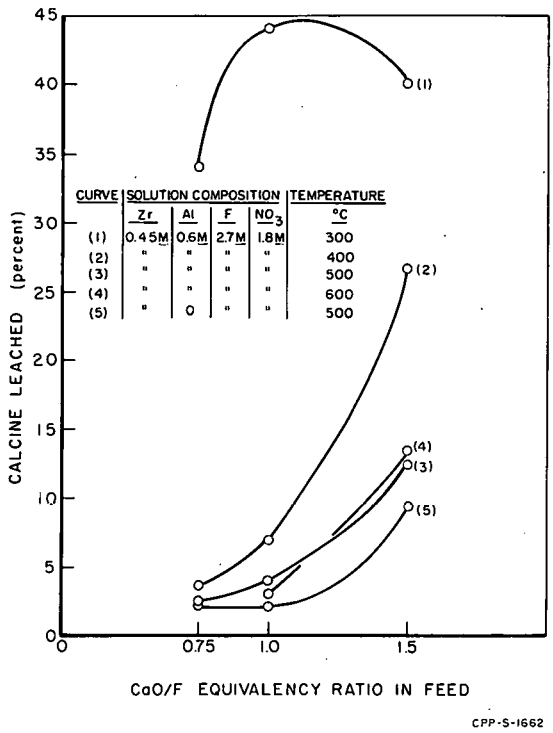

Fig. 13 - Effect of Calcination Temperature and CaO/F Equivalency Ratio on Calcine Leachability

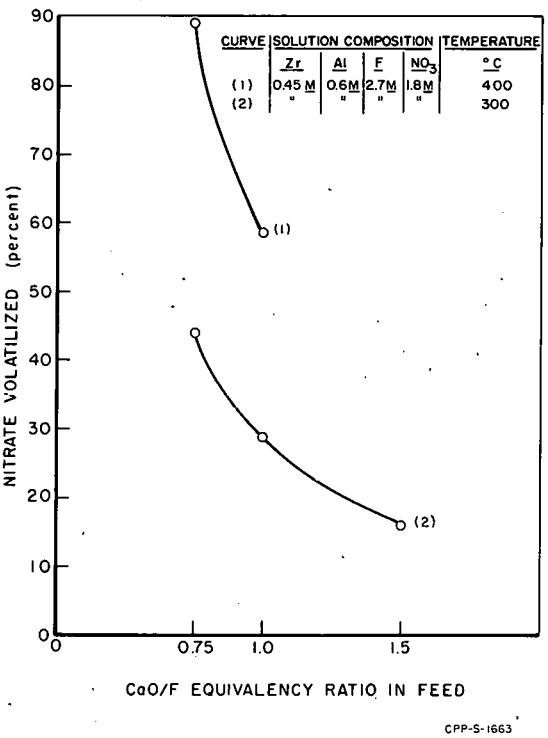

Fig. 14 - Effect of Calcination Temperature and CaO/F Equivalency Ratio on Nitrate Volatilization

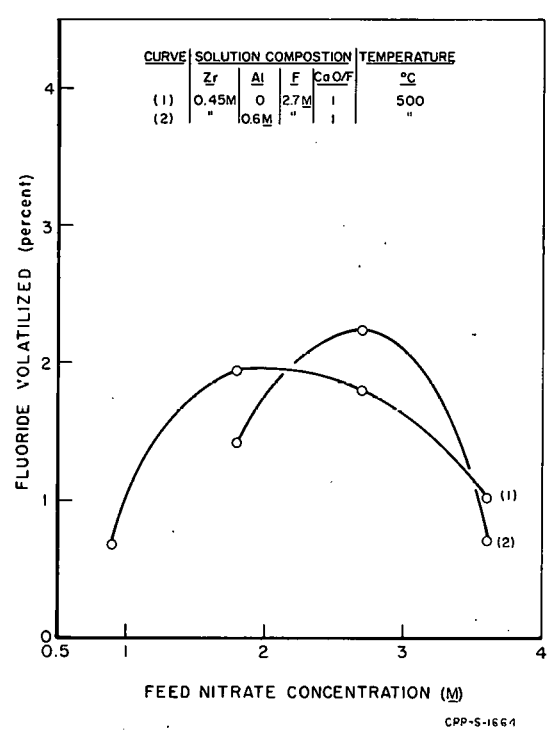

Fig. 15 - Effect of Nitrate Concentration on Fluoride Volatilization

Discussion

The experiments described here allow selection of optimum ranges of the reaction conditions with respect to volatilization of fluoride and calcine leachability. These are: calcination temperature near 500°C, CaO/F equivalency ratio of 0.75 to 1.0, aluminum concentration above 0.3 M, and nitrate concentrations either below 2M or above 3M. Other factors such as digestion time between precipitation and calcination, the rate at which the temperature is raised to calcination level, and the effects of flash drying should be investigated in future work.

The behavior of fission products in this system is a matter of concern, and will be studied, as also will the corrosion aspects of the process.

C. Demonstrational Waste Calcining Facility: Section Chief, J. I. Stevens

Program Planning and Data Correlation: B. M. Legler, Problem Leader; G. E. Lohse and G. J. Raab

Technical Surveillance; L. T. Lakey, Problem Leader; E. J. Bailey, P. N. Kelly, J. L. Lockard and E. A. Travnicek

Construction of the Demonstrational Waste Calcining Facility was not completed during this period as scheduled; present status is estimated at 98 per cent complete, and selected process components have been released for functional testing.

The following paragraphs summarize the work accomplished during the period of this report.

Startup and Standard Operating Procedures

The development of operating procedures was continued in collaboration with Operations personnel. Preliminary drafts of procedures for individual equipment items, plant startup, normal operation, and shutdown have been completed. A procedure for the integrated cold runs was prepared and is being evaluated. Preliminary data sheets for routine operation were prepared and distributed for review.

Additions and Modifications

Several additions and modifications to the facility have been approved and are being designed by the architect-engineer. These include: (1) a pipe line from the chemical make up area of the ICPP to the Waste Calcining Facility for transfer of chemicals (nitric acid and aluminum nitrate) from bulk storage; (2) additional air purge connections to equipment decontamination headers; and (3) a permanent off gas sampling and activity monitoring station for installation in the off gas line before discharge of the gases to the plant stack.

Functional Testing of Equipment

Functional tests of the various pieces of equipment temporarily released by the construction contractor were performed and numerous deficiencies such as improper piping, leaking valves, dirt in equipment, and overheating of blower bearings were discovered. These equipment deficiencies will be remedied by the construction contractor.

NaK Hazards Evaluation

A study of the hazards which might occur through the accidental release of NaK into the calciner or the NaK heater showed that ample time is available for remedial action by the operator before destruction of equipment could occur. The possibility of such a release occurring in the calciner is judged to be very remote since the simultaneous rupture of two pipe walls would be required. Since the NaK heater is installed in a room separated from the remainder of the building by fire walls any accidental discharge of NaK would be confined to a small area.

Quench Solution Pumps

The Johnston deep-well-type pumps previously chosen for circulation of quench and regeneration solutions will be replaced by Lawrence pumps which are now being procured. The latter pump used a heavy shaft to avoid bearings or packing in the pump impeller zone. Bearing material tests are being conducted and promising results appear for boron carbide; however, mechanical design problems are magnified by this brittle material.

Off Gas Sampling

Equipment is being purchased for installation of temporary sampling stations in the off gas system to determine the solids loadings during the cold and hot spike runs. This equipment will be used to define performance of the off gas equipment and to provide information which will be used in determining whether radioactivity in the off gas is removed to the level required by the Radioactivity Concentration Guide.

Feed Nozzle Testing

Liquid feed will be introduced into the four-foot diameter demonstrational fluid bed calciner through two of three Spraying Systems Company, Type 1/2 J, pneumatic atomizing nozzles, a cross section of which is shown in Figure 16. Recent tests with one of these nozzles in the 24-inch square calciner at the Chemical Engineering Laboratory has revealed that severe erosion (0.86 in/yr) occurs on the inner radial 1/3 of the titanium air nozzle faces. The erosion rate is taken as the maximum amount of metal removed in this zone as measured against the surface of the outer radial 2/3 of the nozzle which suffers no detectable erosion. Since this nozzle tip is in direct contact with the fluidized solids, it is postulated than an air vortex at this point results in impingement of particles of alumina at high velocities on the surface. Replacement of the titanium tip with one of type 347 stainless steel reduced the yearly erosion rate by approximately one-half, as shown in Table 8. Both tests were made with approximately the same volume of

TABLE 8

FEED NOZZLE DESIGN AND WEAR RATE

Run	Description	Pertinent Dimensions	Erosion Rate
1A	Titanium flat-faced nozzle flush with calciner wall	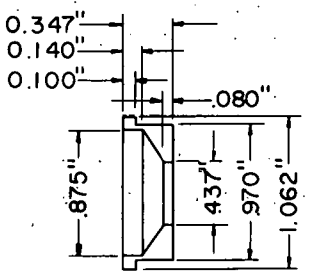	0.86 inch/year (259 hours operation)
1B	Stainless steel-347 flat-faced nozzle flush with calciner wall		0.442 inch/year (150 hours operation)
1C	Aluminum 6061T-6 flat-faced nozzle flush with calciner wall		8.1 inches/year (8 hours 39 minutes oper.)
1D	Aluminum 6061T-6 120° diverging cone extending 0.153 inches into calciner bed	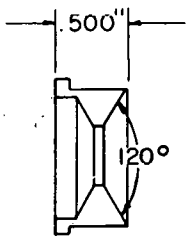	Appreciable (Unable to measure) (7 hours 20 minutes oper.)
1E	Aluminum 6061T-6 flat-face extending 1.645 inches into calciner bed	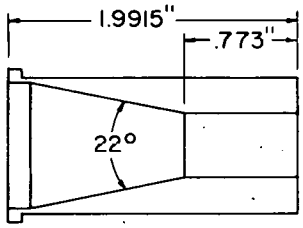	3.37 inches/year (7 hours operation)
1F	Aluminum 6061T-6 22° converging cone extending 1.645 inches into calciner bed	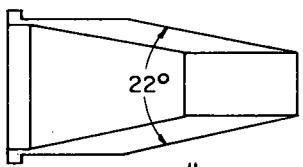	Negligible wear rate (machine marks still visible) (7 hours operation)
1G	Aluminum 6061T-6 22° diverging cone extending 1.203 inches into calciner bed	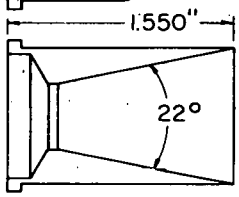	Negligible wear rate (machine marks still visible) (7 hours operation)

Note: All diametrical dimensions not shown are identical with 1A.

CPP-S-1659

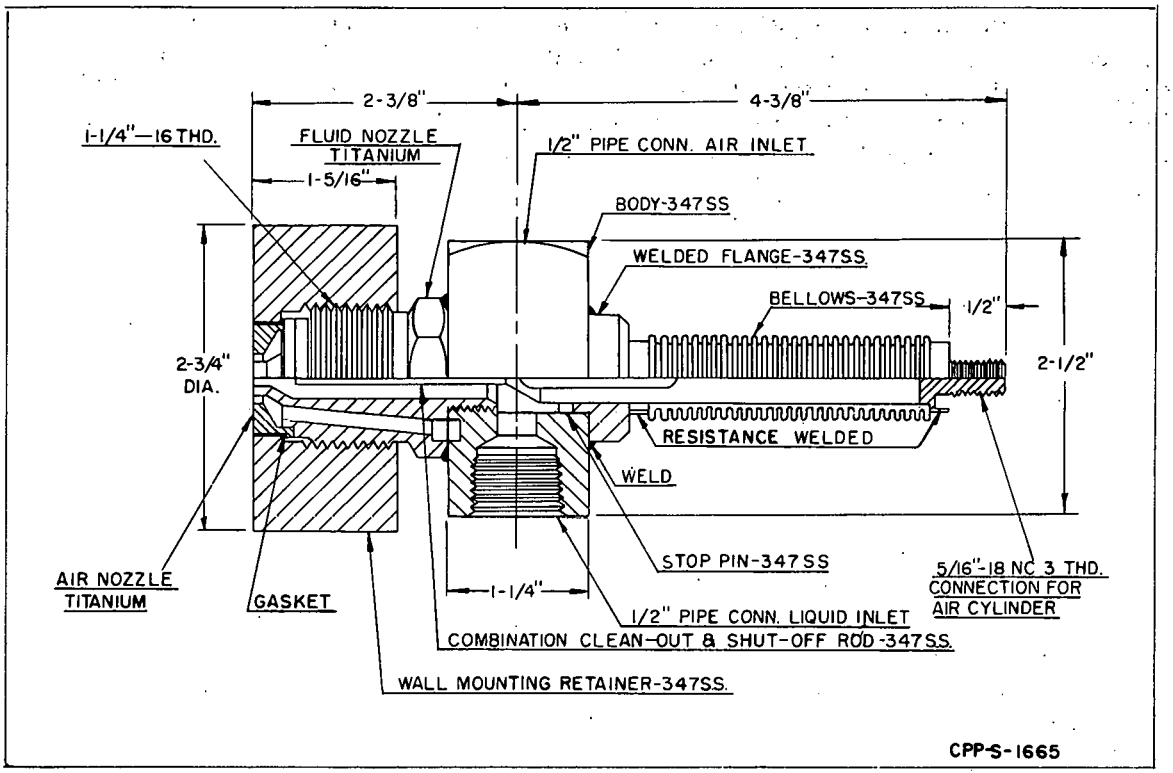

Fig. 16 - Cross Section of Pneumatic Atomizing Nozzle (Spraying Systems Company, Type 1/2 J, with combination clean-out and shut-off needle)

atomizing air; however, the liquid feed rate, bed temperature, and length of operation were considerably different in the two tests.

An aluminum nozzle identical in design to the titanium and stainless steel nozzles was constructed to determine if a test of 7 to 9 hours duration with a nozzle of this softer metal would give accelerated erosion rates, suitable for comparison, when tested in an unheated bed with no liquid feed. This aluminum test nozzle gave high erosion rates (test 1C, Table 8) and the same erosion pattern as when liquid feed was used with the titanium and stainless steel nozzles, indicating that the test method would be valid. Therefore, to study the effect of tip shape on the erosion rate, four tips of various designs (Table 8) were machined from 6061T-6 aluminum and tested in the same manner. Two of the tips (1E and 1F in Table 8) were used with a brass plug to simulate an extension of the liquid orifice to the nozzle tip face. The fluidizing air rate was maintained at 0.78 feet per second and the atomizing air rate adjusted to correspond with an air-to-feed volumetric ratio of approximately 500 at a liquid feed rate of 80 liters per hour. Erosion measurements on each tip were made with a micrometer and then converted to an equivalent yearly erosion rate for comparison purposes. Description of the tips and results of the tests are shown in Table 8.

Based on a comparison of erosion rates, the converging and diverging extended cone (1F and 1G) tips gave the best performance. These designs will be fabricated of stainless steel and tested in the 24-inch calciner using a heated bed and liquid feed. A search for harder materials suitable for nozzle tips is also underway.

V. NEW WASTE TREATMENT METHODS

Section Chief: D. W. Rhodes

The long range program in radioactive waste management at the ICPP aims to reduce waste volumes to a minimum, store wastes as non-leachable solids, separate the non-radioactive alloy components from the fission products, and follow tank corrosion where liquid wastes are stored in temporary tanks. Toward these goals, results are presented on the specific removal of cesium from gross waste by adsorption on ammonium phosphomolybdate, fixation of calcined alumina in a slug of aluminum metal, absorption of gross liquid waste on silica gel followed by calcination, preparation of an insoluble strontium fluozirconate, and the determination of process chemistry of the mercury cathode removal of iron, nickel and chromium from stainless steel wastes.

A. Removal of Long-Lived Radioisotopes from Waste Solutions: M. W. Wilding

Earlier research[5] indicated that ammonium phosphomolybdate (APM) was highly selective for cesium in the presence of ions such as sodium, potassium, aluminum, and hydrogen, which normally interfere in an ion exchange reaction. Additional research during this report period indicated that the capacity of APM was approximately 35 mg of cesium per gram of APM for an $Al(NO_3)_3$ - 0.1N HNO_3 feed. This was about 1.7 times greater capacity than was obtained for an $Al(NO_3)_3$ - 1.0N HNO_3 feed in earlier experiments[5]. In addition, equilibrium data indicated that the relative abilities of H_2O and HNO_3 solutions to dissolve cesium phosphomolybdate (CsPM) during a 24-hour contact was in the order H_2O < 0.1N HNO_3 < 1.0N HNO_3; however, upon longer contact this order was reversed since the solubility of CsPM was about twice as high in H_2O as in 0.1N HNO_3 after 168 hours contact.

Experimental Methods

The APM used in the column experiments was precipitated from solution onto a silica gel carrier. The resulting granular material was about 23 weight per cent APM. The solutions, containing 2M $Al(NO_3)_3$, 0.1N HNO_3, 60 mg of Cs/liter and Cs-137 tracer, were passed upflow through glass columns containing APM at a flow rate of about 5 gal/(ft^2)(hr). The flow rate was limited by the size of the equipment available for continuous collection of the effluents. A constant flow rate was provided by the use of a small pump, and approximately 100 ml fractions of the effluent were collected by means of an automatic fraction collector. The concentration of cesium in the solutions was determined by a gamma counting technique and the concentration of APM by X-ray fluorescence analysis.

Solubility data were obtained by placing samples of the CsPM from the column adsorption experiments into flasks containing water, 0.1N HNO_3, 1.0N HNO_3, and the same solutions saturated with APM. Samples of the solutions were removed periodically and the concentration of cesium in the effluents was determined.

Experimental Results

Analysis of the column effluents indicated that the decontamination factor for cesium was approximately 3 x 10^3 which was near the detection limit for the level of Cs-137 that was used as a tracer. The column capacity as determined from the 50 per cent breakthrough point ($C/C_o = 0.5$) was about 65 column volumes. This corresponded to a capacity of 35 mg of cesium per gram of APM. Approximately 32 per cent of the APM was dissolved during the experiment. The breakthrough curve and a curve showing the concentration of dissolved APM in the column effluents are shown in Figures 17 and 18. The breakthrough curve in Figure 17 was similar to that obtained earlier[5] using 1.0N HNO_3 in the feed solution except for the indicated greater capacity. However, the measured concentrations of APM shown in Figure 18 resulted in a broad "elution curve" whereas the same kind of measurements for the column involving 1.0N HNO_3 in the feed[5] was at a maximum in the initial effluents and decreased gradually. No explanation for this difference is apparent.

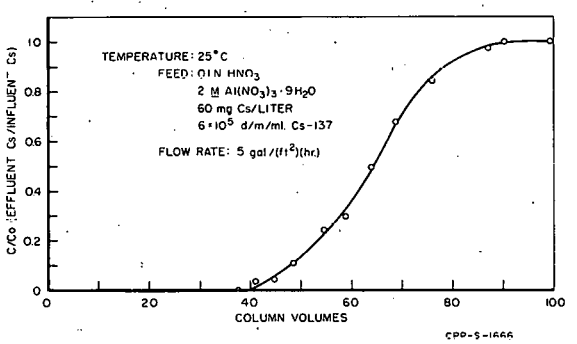

Fig. 17 - Breakthrough Curve for Cesium Adsorption on an APM-SiO_2 Column

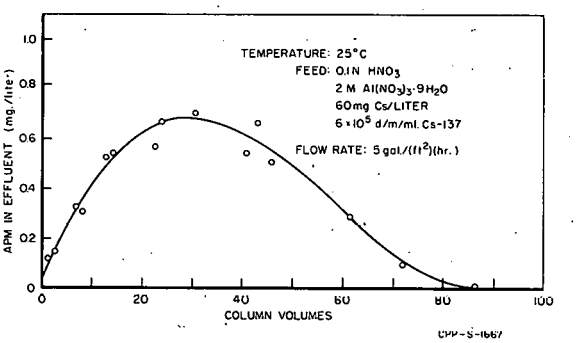

Fig. 18 - Concentration of APM in Effluent from an APM-SiO_2 Column

The equilibrium solubility data are given in Table 9. It is of interest to note that the solubility of CsPM in HNO_3 (0.1N to 1.0N) or water saturated with APM was as little as one-third of the solubility for CsPM in HNO_3 or water alone. Another point of interest involved the concentration of cesium in the column effluent from an adsorption run (0.02 mg Cs/liter) vs the equilibrium solubility of CsPM (>1 mg/liter) for similar solutions and contact times. The much lower concentration of cesium in the column effluents suggests that although the low solubility of CsPM may be an important factor in removing cesium from solution, an additional mechanism such as ion exchange is necessary to reduce the cesium concentration to the low values found in the column experiments.

TABLE 9

SOLUBILITY OF CESIUM PHOSPHOMOLYBDATE IN VARIOUS REAGENTS
(mg of cesium per liter at 25°C)

Time Hrs.	H_2O	H_2O sat'd with APM	0.1N HNO_3	0.1N HNO_3 sat'd with APM	1.0N HNO_3	1.0N HNO_3 sat'd with APM
24	0.99		2.03		4.12	
48	1.90	1.36	2.73	1.23	5.31	4.37
72	2.90	1.62	2.89	1.45	5.30	4.36
168	5.50	1.72	2.87	1.54	6.30	3.96
230	5.15	1.75	2.27	1.67	5.31	3.51
324	5.80	1.69	2.28	1.64	5.41	3.13

Experimental Results (continued)

The optimum use of APM to remove cesium from acid wastes apparently is a function of the rate of dissolution of APM vs the rate of adsorption of cesium from solution by the APM for a given type of waste solution. A series of experiments will be required, using various flow rates through APM exchange columns, to obtain the optimum flow rate for maximum loading with cesium. This maximum very likely will be higher than the values obtained in the few column experiments that have been run to date.

B. Fixation in Stable Solid Media: M. W. Wilding

One approach to the permanent disposal of highly radioactive wastes is converting the waste to a granular solid and imbedding the granules in a stable solid matrix having high thermal conductivity and low leachability. A stable solid was prepared in the laboratory by "fixing" calcined alumina containing cesium-137 in aluminum metal. Subsequent leaching tests indicated that the cesium was leached very slowly from the matrix as compared to the leachability from aluminum oxide alone, but that the leaching rate was rapid compared to the half life of cesium-137.

In other experiments it was demonstrated that silica gel could be used to absorb synthetic liquid waste and the waste calcined in situ. By repeated absorption-calcination cycles, a waste containing 2M $Al(NO_3)_3$ was concentrated fivefold without plugging the pores between the silica gel granules, which were then imbedded in a metal matrix.

Experimental Methods

The calcined alumina containing cesium-137 was placed in a stainless steel tube, one end of the tube inserted into a bath of molten metal, and a vacuum applied to the open end of the tube to fill the interstices with molten metal. After cooling a section was cut from the tube so as to leave two exposed ends and was leached continuously with distilled water at about 80°C. Samples were removed periodically to measure the concentration of cesium in the leachate.

The silica gel for the liquid absorption experiment was contained in a glass column. Liquid was drawn into the column by vacuum, allowed to drain, and the column and its contents heated to 500°C for 2 - 3 hours. This cycle was repeated several times, and the interstices were then filled with metal as described above.

Experimental Results

The results of leaching the calcined alumina-aluminum metal slug containing cesium-137 are shown in Figure 19. This test was intended to simulate leaching after corrosion had penetrated the metal container. Although the leaching rate decreased to a negligible amount after about 600-700 hours, approximately 40 per cent of the total cesium-137 had been removed indicating considerable penetration into the slug through the calcined particles. These data indicate that the porosity of the metal oxide particles is important in determining the leachability of the metal-metal oxide system. The cesium-137 in the calcined alumina granules apparently can be slowly leached from the inside of the slug because of movement of the water through the voids in the calcined alumina. Although the leaching rate is slow relative to the leaching rate from calcined alumina alone (>70 per cent in 1 hour), it is rapid compared to the half-life of cesium-137 (30 yrs).

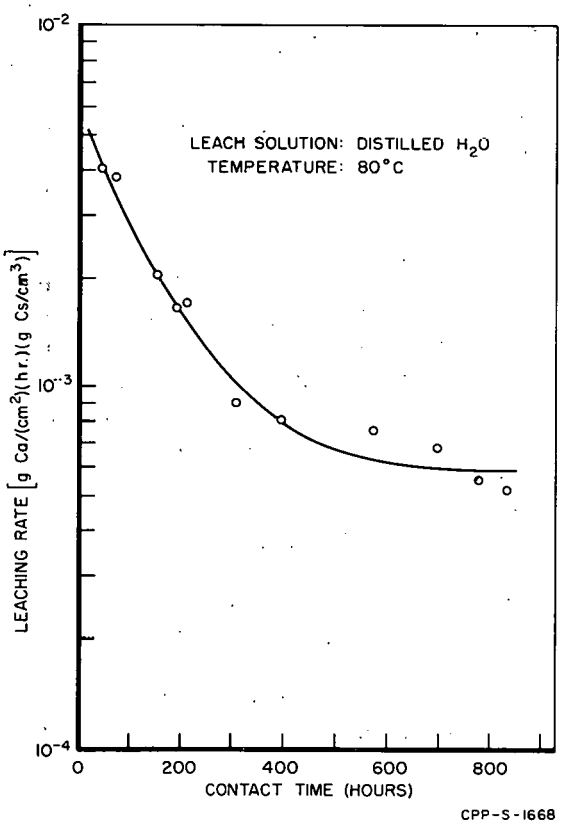

Fig. 19 - Removal of Cs from Alumina Embedded in Al Metal by Leaching With Water

The absorption of synthetic liquid waste by silica gel provides a method of progressing from a high specific activity liquid waste to a granular solid suitable for fixation in metal with a minimum of handling of the liquid and solid. The leachability of the product when exposed to water has not been determined.

C. Preparation of Calcium and Strontium Fluozirconates:
R. L. Hickok, Problem Leader; R. A. Woodriff and D. R. Anderson

This investigation was initiated to furnish basic data to the zirconium-fluoride waste precipitation-calcination program. The principal objective was to prepare and measure the properties of pure compounds of calcium, zirconium, fluorine and oxygen which might be formed in the calcination process. Extension of the work to include preparation of strontium analogues resulted from the discovery that a calcium fluozirconate, $CaZrF_6$, exhibited very low solubility and offered promise that a method might be found to precipitate strontium from wastes in a similar chemical form.

Experimental Method and Measurements

Several methods were used in preparing solids containing calcium or strontium and zirconium and fluorine. In two cases analyses showed the existence of integral atomic ratios which, when correlated with X-ray powder diffraction patterns, indicated relatively pure crystalline compounds. These two compounds were obtained by precipitation when a solution of either calcium nitrate or strontium nitrate was added to a nitric acid solution of fluozirconic acid, H_2ZrF_6.

A large number of preparations were made by other methods and were subjected to X-ray diffraction analysis. A few of these appeared to be relatively pure compounds that have not previously been reported.

Experimental Results

Several crystalline compounds were isolated in varying degrees of purity as shown by X-ray diffraction powder patterns. Elemental analyses were obtained for two compounds which were apparently quite pure and gave integral values for atomic ratios. These two cases are significant in that they represent first preparations of calcium fluozirconate, $CaZrF_6 \cdot (2\text{-}3)H_2O$, and strontium fluozirconate, $SrZrF_6$. The atomic ratios obtained experimentally were $Ca_{1.04}ZrF_{5.92} \cdot 2.7H_2O$ and $Sr_{1.03}ZrF_{5.93}$. The principal X-ray diffraction lines for these compounds are given in Table 10. Several of the other preparations gave unique diffraction patterns which differed from those of any known compounds. Until more analytical data become available, possibly subject to the development of new analytical techniques, identification of the compounds by chemical formula is not possible.

TABLE 10

PRINCIPAL LINES OF X-RAY DIFFRACTION PATTERNS
FOR TWO FLUOZIRCONATE COMPOUNDS

$CaZrF_6$		$SrZrF_6$	
d Angstroms	Relative Intensity	d Angstroms	Relative Intensity
11.0	100	3.80	100
7.01	46	3.10	49
6.57	73	3.08	44
5.49	35	2.72	11
5.15	25	2.07	14
5.06	21	2.04	42
3.66	22	2.02	35
3.44	51	1.90	46
3.37	32	1.72	15
3.25	25	1.69	19
2.83	25	1.63	16
2.33	22		
2.04	32		
1.85	21		

D. Mercury Cathode Electrolysis of Stainless Steel Wastes:
R. L. Hickok, Problem Leader; D. R. Anderson

Mercury cathode electrolysis is being studied as a method for removing iron, nickel and chromium from waste solutions resulting from processing stainless steel reactor fuels. Two phases of this work have been completed. The first was a preliminary scoping study which demonstrated that iron, nickel and chromium could be removed from solutions of interest[2]. The second phase was a polarographic study of the more important fission product elements to determine what conditions would be required to prevent their transfer into the mercury phase together with the base metals[3,5]. Previous reports have discussed the majority of the polarographic results and have described in detail the experimental procedures used. Continued polarographic work carried out during the current reporting period involved an investigation of the behavior of ruthenium.

The objective of a third phase of this project is investigation of those aspects of the process which determine its applicability and practicability. These aspects include base metal removal rate, mercury loading capacity and handling characteristics, current requirements, solution composition requirements, maximum achievable decontamination from long-lived fission products, treatment required to separate the base metals from the mercury and to recover the mercury for re-use, and what, if any, special treatment or techniques will be necessary for permanent storage of the separated metals.

The first problem considered in this phase of investigation was that of loading capacity and handling characteristics of the mercury phase. A second problem, started but not completed, was that of rate of electrolysis.

1. Polarographic Investigation of Ruthenium

The polarographic experiments with ruthenium were carried out using apparatus previously described[2] except that the saturated calomel reference electrode was replaced with a mercury-mercurous sulfate-saturated potassium sulfate electrode with a saturated potassium sulfate-agar plug bridge. The potential of this electrode is +0.40 volts with respect to the saturated calomel electrode, and the data presented have been normalized accordingly to refer to the saturated calomel electrode.

Study of ruthenium in the chloride-free sulfate system showed removal of the element from solutions of potassium sulfate at all potentials above -0.4 volts vs the standard calomel electrode. The rate of removal increased rapidly at potentials above -1.8 volts. The results shown in Figure 20 are essentially identical for solutions in which the concentration of ruthenium is either at tracer level or at 10^{-4} M. No ruthenium was carried into the mercury from a solution of "simulated waste composition"; however, the true fate of ruthenium must be determined with an actual waste solution because of the difficulty of producing the proper ruthenium species in solution.

2. Amalgam Characteristics of Iron, Nickel and Chromium

Preparation of iron, nickel and chromium amalgams for the investigation of amalgam characteristics was carried out using a Bolger electrolysis vessel, Figure 21. The cathode pool consisted of 15 to 20 ml of mercury, and the anode was a one-inch diameter platinum screen. About 200 ml of a 0.2M iron sulfate (or other metal sulfate) solution was placed in the vessel. The mercury-aqueous interface was stirred either with a magnetic stirrer floating on the mercury or with an externally rotated glass stirrer. A battery charger was used to supply

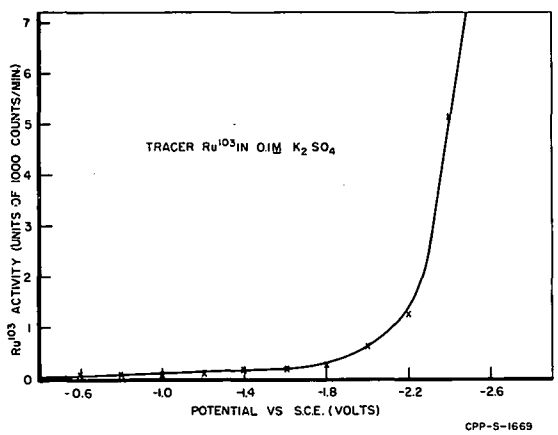

Fig. 20 - Polarographic Investigation of Ruthenium

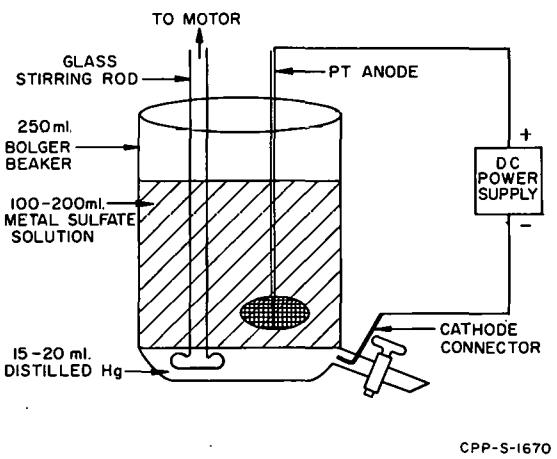

Fig. 21 - Bolger Electrolysis Cell for Amalgam Preparation

6 volts D.C. to the cell. No attempt was made to control the temperature of the solution which rose to as high as 40°C on occasion.

The maximum amount of iron or nickel which could be electrolyzed into the mercury without solidification was about 3 weight per cent. The iron amalgam was a magnetic, lumpy, semi-solid fluid which became more fluid on prolonged standing. The nickel amalgam was a smooth, thixotropic semi-solid. The most concentrated chromium amalgam which could be prepared was 0.3 weight per cent chromium. The limitation on the chromium was not posed by the physical nature of the amalgam but by an inability to electrolyze more chromium. This amalgam was the only one of the three which appeared to be unstable as evidenced by separation from the mercury as a fine black powder.

3. Metal Electrolysis Rate

Measurement of the rate at which the metals can be electrolyzed has been initiated using an Eberback DynaCath apparatus. Deposition rates are being measured as a function of cathode potential and solution composition. Cathode potential is measured using a saturated calomel electrode positioned very close to the mercury surface. The region of cathode potential being studied is below -1.8 volts vs the saturated calomel electrode. Approximately -1.8 volts is considered the maximum voltage which may be used in process application due to polarographic evidence that fission product transfer can be expected to occur at higher voltages. To verify the cathode potential measurement, and to confirm the expected behavior of fission products in the system, strontium-85 tracer is added to the solutions being electrolyzed and the mercury is periodically checked for radioactivity. Analytical results are not yet available.

VI. ELECTROLYTIC DISSOLUTION SYSTEMS

Section Chiefs: H. T. Hahn, Chemical Research
K. L. Rohde, Process Chemistry

The electrolytic dissolution of metallic nuclear fuels shows promise as a universal head-end step in the processing of a wide variety of metals and alloys. Previous studies showed the applicability of electrolytic dissolution to decladding of UO_2 fuel; this report gives results on the electrolytic sectioning of long fuel elements prior to leaching the UO_2 core.

Flowsheet application of electrolytic dissolution has been made to a wide variety of stainless steel and other alloys. A surprisingly small insoluble residue was noted from a number of alloys containing appreciable quantities of molybdenum, silicon or tungsten. Continuous dissolution was demonstrated on a variety of sizes and shapes of several stainless alloys.

Basic studies on the electrolytic process are continuing. Potential-current density relations of electrodes in nitric acid will serve to define the reaction mechanism, to select optimum operating conditions and to select materials of construction. The effect of cell and electrode geometry on the current density distribution is being determined.

The choice of niobium as an anode material has been well established. The cathode material is equally important and may justify a cheaper material of construction. Carpenter 20 cathodes may have applicability under restricted conditions of current density and acid concentration.

The electrolytic dissolution of zirconium alloys has been demonstrated in a non-aqueous electrolyte composed of HCl-methanol. The data on the current density of cathode and anode have been summarized into a single mathematical expression.

A. Electrolytic Dissolution of Stainless Steel in Nitric Acid

1. Survey of Applicability to Metals and Alloys:
J. W. Codding, Problem Leader; M. W. Roberts

Electrolytic dissolution of stainless steel in nitric acid has been extensively studied as an operation in the recovery of uranium from stainless steel fuels. The ease with which the components of stainless steel are put into solution, the stability of such solutions, the desirable corrosion characteristics, and many other factors make electrolytic dissolution an operation of considerable interest for stainless steel fuel processing.

There are many elements which form stable nitrate solutions. More than half of the elements have nitrates that are stable in neutral and acidic solutions. Most of these elements dissolve easily in nitric acid. Some, however, are resistant to nitric acid and impart their resistance to alloys of which they are components. Those which find frequent

use in reactor fuels are aluminum and chromium. Other elements which may be components of fuel alloys and form stable nitrate solutions are cobalt, copper, iron, magnesium, nickel, thorium, uranium, and yttrium. Some elemental components that do not form stable solutions are boron, carbon, hafnium, molybdenum, niobium, silicon, tantalum, titanium, vanadium, tungsten, and zirconium. Manganese forms stable solutions only in dilute nitric acid. It may be seen than many alloys that possess superior strength and resistance to oxidizing, corrosive environments have major components belonging to the first group with minor additions or inclusions of elements of the second group. It is probable that all such alloys can be dissolved electrolytically in nitric acid with the production of minor quantities of insoluble elements and oxides.

An experimental survey has been made to study the applicability of an electrolytic dissolution process to a wide variety of commercially available alloys. The alloys were selected on the bases of: (1) use or proposed use in reactor fuel materials, (2) interesting compositions from the standpoint of insoluble materials, and (3) possible resistance to electrolytic dissolution.

The metals and alloys listed in Table 11 were selected as representative samples for testing. Each material was suspended as the anode in 8M nitric acid and electrolytically dissolved to a solution concentration of 75 gm/l. A current density of approximately 1 amp/cm^2 was used in each case; copper coulometers provided an accurate measure of total energy consumption. At the end of each run, the undissolved residue was separated, dried and weighed, and in some cases analyzed as shown (Table 11).

The results indicate that electrolytic dissolution in nitric acid has a wide range of applicability to a variety of alloy metals. Concentrations of 75 gm/l of each of these metals are easily attained at high current efficiencies, except in the cases of Duriron and Durichlor; with long dissolution times, these two could undoubtedly also be dissolved.

Silicon and molybdenum contributed to excess anode sludge formation but, in general, the amounts of residue remaining after dissolution were not intolerable. The apparent high current efficiencies found for aluminum and aluminum alloys were no doubt due to the action of a certain amount of chemical dissolution during the electrolytic reaction.

2. Bench-Scale Continuous Electrolytic Dissolution: M. W. Roberts

Additional runs have been performed using the small continuous electrolytic dissolver described previously(5). In an effort to circumvent the effects of growth of an oxide film on the "valve metal", a tamping device was arranged to periodically impose a sudden pressure on the stainless steel contents of the dissolver, thus breaking the oxide film. This tamping pressure was conveyed to the dissolving metal through a niobium rod and piston entering the top of the dissolver. Operating conditions and experimental results are shown in Table 12. It is apparent that continued application of emf is not detrimental to electrolytic action if the valve metal film accumulated thereby can be broken by some physical means; tamping seems to be an effective method for accomplishing this.

TABLE. 11

APPLICABILITY OF ELECTROLYTIC DISSOLUTION IN NITRIC ACID TO VARIOUS ALLOYS

	Calculated Current Utilization (gm/amp hr)	Experimental Current Utilization (gm/amp hr)	Current Efficiency (per cent)	Residue	
				Weight % of Dissolved Mass	Spectrographic and X-Ray Characterization
Chromium	0.324	0.333	102.8	0.4	
Inconel X	0.752	0.742	98.6	0.3	
Carpenter 7-Mo	0.532	0.544	102.0	1.65	Cr, Fe, Ni; x-ray shows carbon iron
Illium R	0.706	0.695	98.5	0.5	Mo; not crystalline
Hastelloy C	0.738	0.742	100.5	9.3	Mo; not crystalline
Type 304 SS	0.598	0.587	98.2	0.3	
Type 347 SS	0.594	0.601	101.2	1.2	
Aluminum	0.335	0.414	123.5	1.0	
Carpenter 20	0.634	0.626	98.9	3.0	Nb, Si; NbC/Nb_4C_3 or NbN
Type 316 SS	0.605	0.598	98.8	0.3	
Type 309 SS	0.572	0.576	100.6	1.5	
Hastelloy F	0.648	0.659	101.7	7.4	Nb, Si; NbC/Nb_4C_3 or NbN and ($FeWC$-Fe_4W_2C)(Fe_3MoC)
Inconel	0.788	0.748	95.0	0.5	
Kanthal D	0.529	0.540	102.0	0.6	
Kanthal Al	0.518	0.540	104.2	0.7	
Nichrome V	0.745	0.742	99.6	0.5	
Nichrome	0.720	0.727	101.0	0.8	
Karma	0.706	0.706	100.0	0.7	Cr,Fe, Ni, Si; $NiMnO_4$ and NiO or CrN
Chromax	0.630	0.634	100.6	0.5	Cr,Fe, Ni, Si; carbon iron
Worthite	0.634	0.579	91.5	0.3	
Durichlor	0.828	0.00117	1.4	---	
Duriron	0.821	0.000925	1.1	---	
Durimet 20	0.634	0.612	96.6	0.3	
Refractaloy 26	0.702	0.691	98.5	0.8	Fe, Ni, Si, Th; $NiMn_2O_4$
X-8001 Fuel Plate	0.364	0.439	120.8	1.1	
Al-Al_2O_3-U Fuel Plate	0.414	0.461	111.3	4.0	

TABLE 12

CONDITIONS AND RESULTS OF
CONTINUOUS ELECTROLYTIC DISSOLUTION IN 8M HNO_3

Material	Reagent Flow (ml/min)	Run Time (hrs)	Current (amps)	Utilization (gm/amp hr)	Current Efficiency (per cent)	Amount Dissolved (gm)	Product Conc. (gm/l)
SS 304 Raschig Rings	3.93	13.75	35	0.633	95.9	305	94.0
Cut Nichrome Wire	4.05	16.0	35	0.870	99.4	487	125.3
Illium Spheres	1.67	17.9	29	0.83	----	432	241*
SS 347 Slugs	3.53	18.4	28	0.650	98.5	335	86.0

* Product Solution was unstable.

3. Electrolytic Sectioning: M. W. Roberts

A number of plans for reprocessing reactor fuels include disassembly of the fuel elements followed by mechanical cutting of the individual fuel pins or rods in order to expose the fissionable material within. This material can then be dissolved or leached from the pin segments by, for example, nitric acid, thus yielding a feed for further purification. The Zircaloy or stainless steel pin segments left from the leaching process would be discarded as a solid waste. Two possibly serious problems of such a procedure are that a fairly powerful mechanical shear or saw must be operated in a remote area, and that chips, dust, and other difficult-to-confine contaminated particles are created by mechanical action. Since electrolytic sectioning appears to circumvent these difficulties, it has been examined as an alternative to mechanical chopping or sectioning.

In electrolytic sectioning, cutting is accomplished by the electrolytic dissolution of a narrow band of the cladding material. A hollow needle cathode delivers a fine stream of electrolyte against the part to be cut. The fuel pin segment is made anodic. Either the fuel pin or the cathodic needle is so moved that the full course of the line to be cut is repeatedly and uniformly covered. Since the products of the cut are dissolved electrochemically, no chips are produced during the operation.

Experimental

The experimental set-up used to demonstrate electrolytic sectioning is shown in Figure 22. A piece of 304 stainless steel tubing was used as the "fuel pin" for sectioning; its wall thickness was 0.17 cm. The weight of the stainless steel tube was sufficient to assure excellent electrical contact between it and the knurled rollers providing rotary movement. A Fisher Minimill was used to rotate the tube being sectioned.

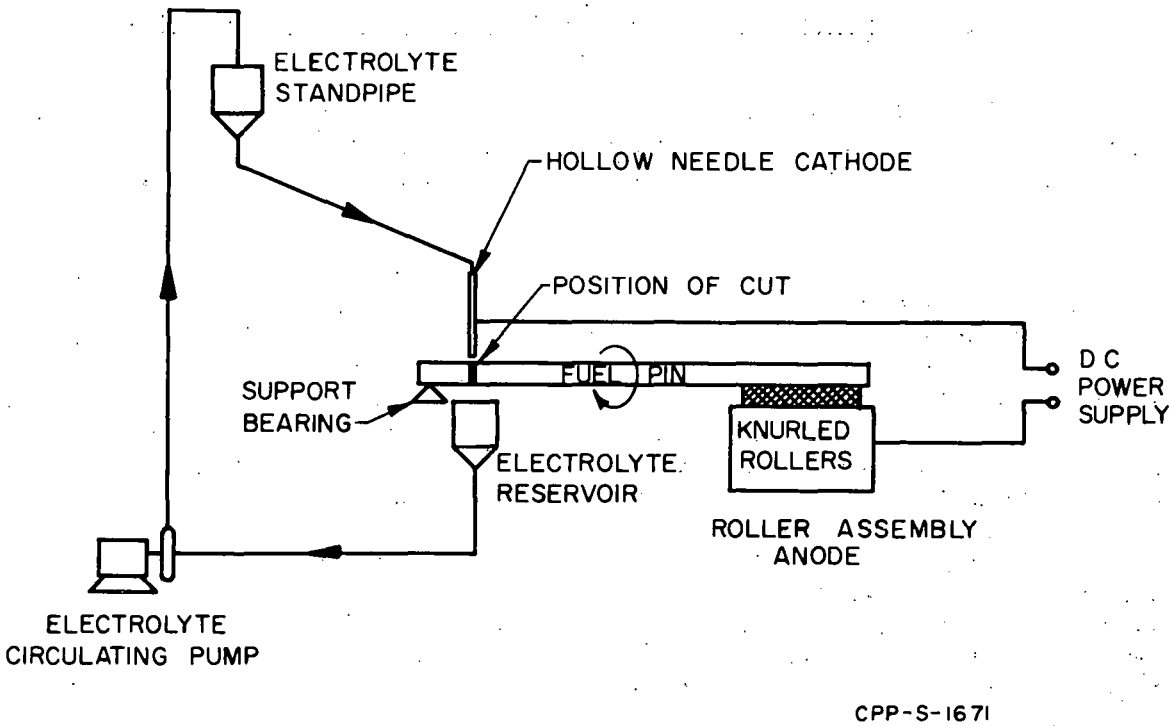

Fig. 22 - Electrolytic Sectioning Device

The hollow needle cathode was a platinum - 10 per cent rhodium tube, 5 cm long, with an outside diameter of 0.318 cm and an inside diameter of 0.159 cm. It was mounted just above the tube and maintained at about one mm distance from the bottom of the cut. Eight molar nitric acid flowed through the cathode and over a portion of the stainless steel tube, eventually falling into the reservoir provided from which it was continuously recirculated.

Results

When a potential of 8.5 volts was applied between the hollow needle cathode and the rotating stainless steel tube, a current of 4 amperes was produced. The tube dissolved in a narrow band traced on its circumference, and parted into two sections in 48 minutes. It had lost 1.98 gms and showed a cut width of about 0.36 cm at the widest point. Current utilization was 0.62 gm/amp hr with a current density between 40 and 70 amps/cm^2 at the tube.

In the system described above, the dissolved metal represents about three per cent of the total cladding weight, if four-inch sections are assumed.

4. Potential-Current Density Relationships in Nitric Acid:
J. R. Aylward, Problem Leader

Potential-current density measurements will be made for metal electrodes in nitric acid in order to define reaction mechanisms, to permit selection of optimum operating conditions, and to evaluate corrosion problems.

A new 750 watt potentiostat-galvanostat has been delivered and tested with a number of cells. Maximum noise and drift were found to be 10 mv peak to peak and 2 mv per hour, respectively. Rise times as short as 20 msec have been obtained. Some ringing is noticeable at currents greater than 3 amps. By placing a large (4,000 μt) capacitor across the main power supply output, higher currents can be obtained before ringing sets in, but an increase in rise time results. Some minor changes in the potentiostat will be made to improve its operation.

Some scoping experiments were initiated on cathode materials suitable for investigation of the reduction of nitric acid. Results of experiments done to date on a number of materials indicate that the reduction is "autocatalytic". In view of this, some revision of experimental approach will be necessary. The course to be followed will be determined on completion of an additional literature survey. These experiments also revealed that zirconium would be unsuitable as a cathode in nitric acid because of its high disintegration rate.

5. Effect of Cell and Electrode Geometry on Current Density Distribution

Current interest in electrolytic dissolution processes requires basic information of the effect of cell and electrode geometry upon current density distribution. Information of this nature is important to electrolytic process cell design and also operational behavior, as for example, the need to maintain a minimum current density. Most cell configurations are sufficiently complex that they are not directly amenable to theoretical calculation. Preliminary attempts to define current path are therefore limited to approximations based upon theory available for the simplest configurations, or upon experimental analog simulation.

a. Variations in Cathode Current Density:
E. M. Vander Wall, Problem Leader; D. P. Pearson

Presently proposed dissolver design consists of fuel elements suspended in a cylindrical anode basket which is concentrically surrounded by a cathode. A study has been made of the effect of anode basket hole arrangement upon effective electrolytic resistance and upon the uniformity of current at the cathode. The resistance is of interest because the I^2R energy dissipated during a dissolution is directly proportional to it. The current variation on the cathode is of concern because, for many electrochemical systems, undesirable side reactions will occur if the local current density exceeds some value characteristic of the system. Since the overall dissolution rate is proportional to the average cathode current density, it is desirable that this average be as large a fraction as possible of the maximum (limiting) current density.

Since no simple method of calculating the effect of hole geometry on solution resistance was available, the effect was studied experimentally. The resistance of an aqueous solution was measured between two electrodes designed to simulate a section of cathode surface and an anode basket hole. Insulating surfaces perpendicular to the planes of the electrodes restricted the current as would the symmetry of repeating holes in an actual anode basket. The resistance values measured were divided by the resistances measured at the same anode-cathode distance with an anode identical to the cathode, i.e., basket is "all holes". This ratio (r) was found to be almost independent of the anode-cathode spacing, and to depend primarily on the ratio of the anode hole diameter to the inter-hole distance. If the inter-hole distance is not greater than the hole diameter, the ratio (r) is less than 2.8.

It should be noted that this value is less than the example value ($\phi = 5$) previously assumed[5], which was based on the ratio of total anode basket area to basket-hole area. In other words, the resistance ratio is between unity and the above area ratio.

No theory is available to calculate exactly the current variation on the cathode. Therefore, a point-by-point summing procedure, which is estimated to be accurate to within two per cent as applied here, was devised to calculate the current at a given point on the cathode. For a given geometry, the average current and the maximum current (directly opposite an anode basket hole) on the cathode were calculated. The ratio of hole diameter, d, to anode-cathode spacing, a, was varied from 0.33 to 3. The ratio of the distance between adjacent hole edges, L, to anode-cathode spacing was varied from 0.33 to 2. The holes were in a square array.

The salient results can be summarized as follows: (1) for the average current to be not less than 90 per cent of the maximum current, $L \leq 1.34\ a - 0.44\ d$, and (2) for the resistance between cathode and anode basket to be not greater than three times the resistance when the basket is "all holes", $L \leq 1.2\ d$.

A less extensive study was made for triangular arrays of holes. The improvements in resistance and current uniformity compared to the square array appear to be less than 10 per cent.

b. Analog Simulation: J. R. Aylward, Problem Leader; R. E. Ohlin

Testing of the electrical characteristics of conductive rubber sheeting for the analog simulation of electrolytic cells is in progress. An abnormal voltage gradient was found to exist in the immediate vicinity of the electrodes. This may arise from an electrode contact resistance. The resistance of the bulk material is uniform within $\pm$ 10 per cent.

6. Corrosion of Carpenter 20 Cathode: K. L. Rohde

The cathode weight loss data for Carpenter 20 in nitric acid, obtained during earlier experiments[2], has been recalculated in terms of penetration and the anodic component of the current at the cathode. These

penetration rates and current components are shown in Table 13 with the nominal cathode current densities, the cell potentials, and the solution compositions. Several trends are apparent. The corrosion increases with the nominal cathode current density, and at the highest current density tested, 1.5 amps per cm^2, the corrosion is greatest in the system where the total nitrate and hydrogen ion are least. These data make it possible to define tentatively the operating regions which must be avoided to prevent experiencing a given level of corrosion. In Table 14 a level of 20 mils per month corrosion was arbitrarily selected and the current densities and solution compositions which could be used without exceeding this limit are shown. The data available do not make it possible to separate the effect due to total nitrate from that due to hydrogen ion, and therefore, both are shown as limiting. These limits are not highly restrictive, although it would be desirable to be able to dissolve to as low an acidity as possible.

TABLE 13

CORROSION OF CARPENTER 20 CATHODE DURING ELECTROLYTIC DISSOLUTION(a)

Exp.No.(b)	Cathode Current Density (amps/cm^2)	Cell Potential (volts)	Solution Composition		Cathode Corrosion	
			Hydrogen (M)	Nitrate (M)	Current Density (ma/cm^2)	Penetration (MPM)
5	0.5	2.8	0.5	4.4	0.09	2
6	1.0	3.9	1.5	4.8	0.5	12
2	1.0	4.1	1.4	4.6	0.6	14
10	1.0	4.1	1.1	4.3	1	23
11	1.0	4.0	1.4	4.6	2	51
4	1.5	6.4	2.0	6.2	0.6	12
3	1.5	7.1	0.9	4.4	7	160
7	1.5	8.1	0.5	4.4	11	250

(a) In each experiment except No. 11, 46-54 g/l of Fe, Cr, Ni as nitrates were present in 18-8 stainless steel proportions. In No. 11, the anode was Carpenter 20 and the solution composition was altered accordingly. Each experiment ran for 4 hours with 23, 46, or 70 g stainless steel dissolving depending on the current density. Experiments 2 and 11 were at 85°C, all others at 101°C.

(b) Experiment numbers are as given in Table 17 of reference 2 (IDO-14512).

TABLE 14

FLOWSHEET LIMITATIONS IMPOSED BY CARPENTER 20 CATHODE CORROSION

(If cathode corrosion rates above 20 MPM are to be avoided, then both total nitrate and hydrogen ion in the dissolver solution must exceed the values given below.)

Current Density Used (amp/cm^2)	Required Concentration in Dissolver Product Solution	
	nitrate (M)	hydrogen ion (M)
0.5	> 4.5	> 0.5
1.0	> 4.5	> 1.5
1.5	> 6.0	> 3.0

The very low corrosion rate at 0.5 amps per cm^2 is encouraging since it suggests that the regions of very low current density, such as at the end of the active cathode area, and in the vessel fittings, will not be subjected to high electrochemical corrosion.

It may be noted that the coupons used in these tests were not polished or finished in any manner, and therefore, were apparently active almost immediately in the solutions. The results obtained here may be contrasted to those described previously[2] wherein the coupons were polished to a 150 grit finish. In the latter experiments, the material did not apparently become active to any appreciable extent.

B. Electrolytic Dissolution of Zirconium in HCl-Methanol

Previous work[2] has demonstrated that zirconium may be dissolved electrolytically in HCl-methanol solutions. Two distinct regions involving different reaction mechanisms have been observed in the potential-current density curves. Below -0.1 volt, measured with respect to the saturated calomel electrode, dissolution with etching takes place and some zirconium remains undissolved as a finely divided residue. At potentials more positive than -0.1 volt the zirconium is electropolished and no residue is produced.

Currently reported work includes an extensive study of the potential-current density relationships for this system as a function of temperature and HCl concentration.

1. Potential-Current Density Relationships for Zirconium in HCl-Methanol: J. R. Aylward, Problem Leader; E. M. Whitener

Additional potential-current density data have been compiled for the zirconium-HCl-methanol system. It can be shown from electrokinetic

theory that the potential-current density curves obtained for a zirconium electrode in HCl-methanol solutions are given by an equation of the form:

$$I = \frac{i'_o \left[\exp(1/b_a \eta) - \exp(-1/b_c \eta)\right]}{1 + \frac{i'_o}{i_e} \exp(1/b_a \eta)} \qquad (1)$$

where I is the cell current density, η the overvoltage, i'_o the rate of zirconium dissolution at zero overvoltage (corrosion current), i_e the limiting current density, and b_a and b_c the anodic and cathodic Tafel slopes, respectively. The corrosion current density is independent of HCl concentration but was found to be a function of temperature as follows:

$$i_o = \exp(20.1 - \frac{\Delta H_c^{\ddagger}}{RT}) \qquad (2)$$

where $\Delta H_c^{\ddagger}$ = 16.6 kcal/mole is the heat of activation for the dissolution reaction under activation control (this is a better value than previously reported[5], but lies within the estimated accuracy of ± 1.6 kcal/mole). The limiting current density for electropolishing was found to be given by:

$$i_e = 2.23\, C^{-0.447} \exp(\frac{\Delta H_e^{\ddagger}}{RT} - 12.65) \qquad (3)$$

where C is the HCl concentration in moles/liter and $\Delta H_e^{\ddagger}$ = 7.4 kcal/mole is the heat of activation for the electropolishing process. Substituting (2) and (3) in (1) along with the values for the Tafel slopes gives:

$$I = \frac{\exp\left[20.1 + (5.80\eta - 8.28)\, 10^3/T\right] - \exp\left[20.1 - (4.22\eta + 8.28)\, 10^3/T\right]}{1 + C^{0.447} \exp\left[6.64 + (5.80\eta - 4.75)\, 10^3/T\right]} \qquad (4)$$

This equation summarizes all the data obtained on the anodic and cathodic behavior of zirconium in HCl-methanol solutions and gives the current density as a function of overvoltage from -0.5 to +3.0 volts, HCl concentrations from 1.5 to 13M and temperatures from 275 to 315°K.

VII. THE ARCO PROCESS - DISSOLUTION OF FUEL ALLOYS IN MOLTEN CHLORIDES

Section Chiefs: H. T. Hahn, Chemical Research;
K. L. Rohde, Process Chemistry

The ARCO process employs molten lead chloride as a solvent for reactor fuel alloys. The product salt contains uranium chloride together with excess lead chloride and the alkali, alkaline earth and rare earth fission products. Satisfactory uranium recovery from the salt matrix has been achieved with HNO_3 leaching.

Work in this quarter has been concerned with HCl leaching of the salt matrix, niobium behavior in lead chloride, solubility of uranium oxide in lead chloride, and some additional corrosion studies.

A. HCl Leaching of the ARCO Salt Matrix:

E. M. Vander Wall, Problem Leader; D. L. Bauer

Dissolution of fuel elements by the ARCO process yields a salt matrix which contains the uranium chlorides. The existing method of uranium recovery (HNO_3 leaching) entails conversion from a chloride to a nitrate system. Since it might be advantageous under some circumstances to avoid this conversion step, a series of experiments was performed in which HCl (0.25M to 12M) was employed as the leaching agent.

Salt matrices were prepared by dissolving enough uranium metal in approximately 0.043 moles of molten lead chloride to produce a solution which contained about 10 mole per cent uranium chlorides. In most cases this product was ground by mortar and pestle, refluxed and stirred for one hour with 10 ml of HCl and then filtered. The solid residue was washed several times with acid of the same concentration. The total volume of wash acid was 15 ml. The acid leaching operation was then repeated. After this, the remaining solid residue was refluxed with concentrated HNO_3 to remove the chloride and then diluted with water until the entire residue dissolved. The three solutions resulting from this procedure were then analyzed for uranium

The results of these experiments are plotted in Figures 23 and 24. In three experiments, 20 ml of HCl was used instead of the usual 10 ml for the leaching steps. This change in volume appears to have no significant effect upon the amount of uranium removed. In two other experiments, the matrices were not ground prior to leaching. However, the refluxing and stirring actions served to pulverize the matrices to a considerable extent. The uranium analyses indicate that grinding the matrices prior to leaching produces no apparent difference in the results when the reflux operation is performed for an hour.

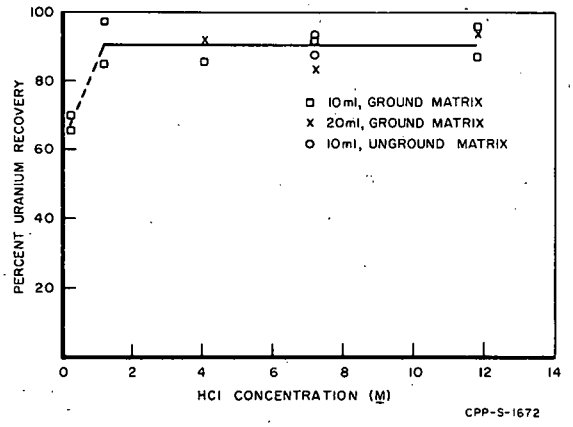

Fig. 23 - Per Cent Uranium Removed by Initial Leach of ARCO Salt Matrix with Various Concentrations of HCl.

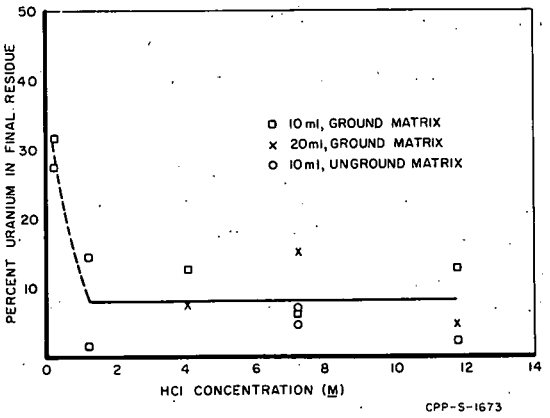

Fig. 24 - Residual Uranium After Two Leaching Operations with Various Concentrations of HCl

Although there is considerable scatter in the data which were obtained, it is obvious that under these experimental conditions HCl is not a suitable leaching agent. The concentration of HCl in the range from 1.2M to the concentrated acid makes no significant difference in the final uranium loss. In all cases, the uranium losses are prohibitive. Comparison with previous work[10] indicated that 8M HNO_3 is a much more satisfactory leaching agent, with an average uranium loss of only 0.04 per cent.

B. Niobium Behavior in Lead Chloride:
E. M. Vander Wall, Problem Leader; J. L. Teague

A program for determining the disposition of the fission product elements niobium and ruthenium in the ARCO process has been initiated. At the present time a number of niobium coupons have been subjected to dissolution in $PbCl_2$ at 600°C. Although all coupons were cut from the same sheet of niobium and have had the same surface treatment, an unpredictable amount of scatter in the results of duplicate runs, and also some discrepancies in results of differing runs, have made calculation of a rate constant impossible. Preliminary observations indicate that the rate increases up to about 1 1/2 to 2 hours contact time, and then becomes constant at approximately 0.06 mg/(cm^2)(min).

Several niobium coupons have been irradiated in the MTR to produce Nb^{94}. These coupons will be used in tracer experiments to determine volatility of $NbCl_5$ from molten $PbCl_2$ systems, and also to determine niobium behavior during acid leaching of $PbCl_2$.

C. Uranium Oxide-Lead Chloride Experiments:
E. M. Vander Wall, Problem Leader; J. L. Teague

To investigate the applicability of the ARCO process to civilian power reactor fuels, the solubility of UO_2 in molten $PbCl_2$ was determined at several temperatures from 520 to 800°C. The UO_2 used was in the form of pellets which were taken from unirradiated PWR fuel pins. In each determination 5.8 g of UO_2 was placed in contact with 10 g of molten $PbCl_2$ at the desired temperature for one hour. In all experiments, the UO_2 pellets gained 1 to 4 mg, and appeared to be insoluble.

One pellet which was kept in contact with $PbCl_2$ for five hours at 800°C gained 23 mg. The $PbCl_2$ melt from this experiment was analyzed and found to contain 0.3 mg of uranium. This loss corresponds to a dissolution rate of 0.3 $\mu g/(cm^2)(min)$. The relative insolubility of UO_2 in molten $PbCl_2$ suggests the feasibility of using the ARCO process as a decladding step for zirconium- or Zircaloy-clad UO_2 fuel elements.

D. Alloy Corrosion Tests: N. D. Stolica, Problem Leader; M. R. Bomar

An additional series of static corrosion tests was completed in the lead-lead chloride system at 528°C. The experimental procedure and earlier results have been reported previously[1,2,3]. In the tests, the specimens were so placed that about one third of the specimen area was immersed in lead, one third in fused lead chloride, and one third in the argon atmosphere of the furnace which contains some lead chloride vapor. Table 15 gives the exposure times and corrosion rates.

TABLE 15

CORROSION OF SELECTED ALLOYS IN THE LEAD-LEAD CHLORIDE SYSTEM AT 528°C

Alloy	Exposure (Hours)	Weight Loss (Mils per Month)
Hastelloy B	336	2.9 - 2.6
Haynes 25	336	1.9 - 2.3
Haynes 36	336	2.7 - 1.3
Haynes 21	336	1.4 - 1.1
Multimet	336	5.6 - 5.1
Multimet	120	4.6 - 4.6
Inor 8	336	3.5 - 4.1
Inor 8	120	3.6 - 3.5
Incoloy 804	120	4.7 - 6.0

These corrosion rates were calculated on the assumption that the attack was general, but in all cases there were varying amounts of localized attack. The Haynes 21 coupons appeared to have the best corrosion resistance to this media. It was noted that all of these materials were very difficult to clean after exposure.

VIII. REPORTS AND PUBLICATIONS ISSUED DURING THE QUARTER

1. Kent, R.A. and Rohde, K. L., Tributyl Phosphate Extraction of Uranium from Ammonium Nitrate Solutions, IDO-14501, July 22, 1960.

2. Paige, B. E., Barium Fluozirconate Precipitation from Hydrofluoric Acid-Zirconium Fuel Reprocessing Solutions, Part I. Process Chemistry, IDO-14511, September 20, 1960.

3. Bordeaux, J. J. and Adams, G. S., Corrosion of Alloys in Aqueous Hydrofluoric-Nitric Acid Solutions, IDO-14516, August 10, 1960.

4. Moffat, A. J., A Potentiometric Study of Zirconium-Nitrate and Zirconium-Fluoride Systems, IDO-14517, August 29, 1960.

5. McLain, M. E. and Rhodes, D. W., Stainless Steel Process Wastes: I. Removal of Alloy Metals From Waste Solutions by Mercury Cathode Electrolysis, IDO-14533, September 30, 1960.

6. Hahn, H. T. and Vander Wall, E. M., Paper, "The ARCO Process - Salt Phase Chlorination of Reactor Fuels". Presented at New York Meeting of ACS in September, 1960.

IX. REFERENCES

1. Stevenson, C. E., Technical Progress Report for July through September, 1959, Idaho Chemical Processing Plant, IDO-14509.

2. Bower, J. R., Idaho Chemical Processing Plant Technical Progress Report, October-December, 1959, IDO-14512.

3. Bower, J. R., Idaho Chemical Processing Plant Technical Progress Report, January-March, 1960, IDO-14520.

4. Paige, B. E., Barium Fluozirconate Precipitation from Hydrofluoric Acid-Zirconium Fuel Reprocessing Solutions, Part I. Process Chemistry, IDO-14511, September 20, 1960.

5. Bower, J. R., Chemical Processing Technology Quarterly Progress Report, April-June, 1960, IDO-14534

6. Moffat, A. J. and R. D. Thompson, The Effect of Extracted Zirconium and Nitric Acid Upon the Chemical Stability of Tributyl Phosphate, (to be published).

7. Slansky, C. M., L. A. Decker, and K. L. Rohde, Classified Report, IDO-14524.

8. Stevens, J. I., Idaho Chemical Processing Plant Technical Progress Report, Radioactive Waste Disposal Projects, January-March, 1960, IDO-14530.

9. Beirne, T., and J. M. Hutcheon, "Physics of Particle Size Analysis", Supplement No. 3 to the British Journal of Applied Physics, London, 1954.

10. Vander Wall, E. M., H. T. Hahn, and D. L. Bauer, Salt Phase Chlorination of Reactor Fuels, II. ARCO Process Definition and Scoping Studies, IDO-14525.

PHILLIPS
PETROLEUM
COMPANY

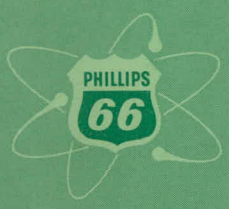

ATOMIC ENERGY DIVISION